

Syntheses and Applications of Symmetrical Dinuclear Half-Sandwich Ruthenium(II)–Dipicolinamide Complexes as Catalysts in the Transfer Hydrogenation of Ketones

Robert Tettey Kumah, Sabathile Thandeka Mvelase and Stephen Otieno Ojwach *

School of Physics and Chemistry, University of KwaZulu-Natal, Pietermaritzburg
Campus, Private Bag X01, Scottsville 3209, South Africa

* Correspondence: ojwach@ukzn.ac.za

Electronic Supplementary data

| Entry | ITEM | Page |
|-------|---|------|
| 1 | Synthesis of N,N'-(1,2-phenylene)bis(pyridine-2-carboxamide): H₂L1 | 2 |
| 2 | Synthesis of N,N'-(4,5-dimethyl-1,2-phenylene)dipicolinamide: H₂L2 | 2 |
| 3 | Synthesis of N,N'-(4-methoxy-1,2-phenylene)dipicolinamide: H₂L3 | 3 |
| 4 | ¹ H NMR spectra data of ligands and Ru(II) complexes (Figures S1-S7) | 3 |
| 5 | ¹³ C NMR spectra of ligands and Ru(II) complexes (Figures S9-S14) | 7 |
| 6 | ³¹ P NMR of complexes Ru2-Ru4 (Figures S15 and S17) | 11 |
| 7 | ¹⁹ F NMR of complexes Ru2- Ru4 (Figures S18 and S20) | 12 |
| 8 | FT IR Spectra of ligands and Ru(II) complexes (Figures S21-S27) | 14 |
| 9 | ESI-MS spectra of ligands and Ru(II) complexes (Figures S28-S34) | 17 |
| 10 | ¹ H NMR spectra of TH aliquots taken at the time/h (Figures S35-S42) | 22 |
| 11 | A plot of Conversion, TOF vs catalyst loading | 27 |
| 12 | Kinetic plot for determination of <i>k_{ob}</i> of the catalysts (Figures S43) | 28 |
| 13. | Molecular structures and packing arrangements of Ru1 and Ru4 | 29 |

1. Synthesis of Phenylene bis(pyridyl-carboxamide) ligands

1.1.1. Synthesis of *N,N'-(1,2-phenylene)bis(2-pyridyl)carboxamide (H₂L1)*

To a solution of pyridine carboxylic acid (0.50 g, 4.06 mmol) in pyridine (10 mL) is added a *o*-phenylenediamine (0.26 g, 2.41 mmol) (0.26 g, 2.41 mmol) and triphenylphosphate (1.00 mL) and refluxed at 110 °C for 6h to form a white suspension. The reaction mixture was cooled to room temperature, 20 ml of distilled water is added and filtered under vacuum to obtained white crude product. The crude is then washed with dry ethanol (30 mL) and dried in vacuum to obtained white crystalline solid. Yield = 0.66 g (86%). ¹H NMR (400 MHz, DMSO) δ_H: 10.71 (s, 2H_{amide}), 8.65(t, ³J_{HH} = 5.6 Hz, 2H_{pyridine}), 8.19 (d, ³J_{HH} = 6.4Hz, 2H_{pyridine}), 8.06 (d, ³J_{HH} = 6.4Hz, 2H_{pyridine}), 7.79(t, ³J_{HH} = 6.4Hz, 2H_{pyridine}) 7.67(m, ³J_{HH} = 6.4Hz, 2H_{benzene}), 7.32(d, ³J_{HH} = 10 Hz, 2H_{benzene}). ¹³C{¹H} NMR (101 MHz, CDCl₃) δ: 163.3, 149.9, 149.0, 138.6, 131.4, 127.5, 126.2, 125.7, 122.9. FT-IR (cm⁻¹): (ν_{C=O})_{amide} = 1664; (ν_{N-H})_{amide} = 3312. ESI-MS, m/z(%): 341[M+Na⁺,100], 659[2M+Na⁺, 60].

1.1.2. Synthesis of *N,N'-(4,5-dimethyl-1,2-phenylene)dipicolinamide (H₂L2)*

A picolinic acid (0.50 g, 3.62 mmol), 4,5-dimethylbenzene-1,2-diamine (0.26 g, 2.41 mmol), triphenylphosphate (1.10 mL) and in pyridine (10 mL) refluxed at 110 °C for 6h. white compound was obtained. Yield = 0.63 g (86%). ¹H NMR (400 MHz, DMSO) δ: 10.17 (s, 2H_{amide}), 8.57 (m, ³J_{HH} = 5.6 Hz, 2H_{pyridine}), 8.31 (m, ³J_{HH} = 4.8Hz, 2H_{pyridine}), 7.91 (m, ³J_{HH} = 4.8 Hz, 2H_{pyridine}) 7.64 (s, 2H_{benzene}), 7.45(m, ³J_{HH}=6.2 Hz, 2H_{pyridine}), 3.71(s, 3H) 2.34(s, 2CH₃). ¹³C{¹H} NMR (101 MHz, CDCl₃) δ: 162.8, 149.9, 148.2, 137.4, 134.8, 127.8, 126.3, 125.7,122.5, 19.8. FT-IR (cm⁻¹): (ν_{N-H})_{amide} = 3325; (ν_{C=O})_{amide} = 1663. ESI-MS: m/z (%): 369[M + Na⁺, 20], 715[2M + Na⁺, 100].

1.1.3. Synthesis of *N,N'-(4-methoxy-1,2-phenylene)dipicolinamide (H₂L3)*

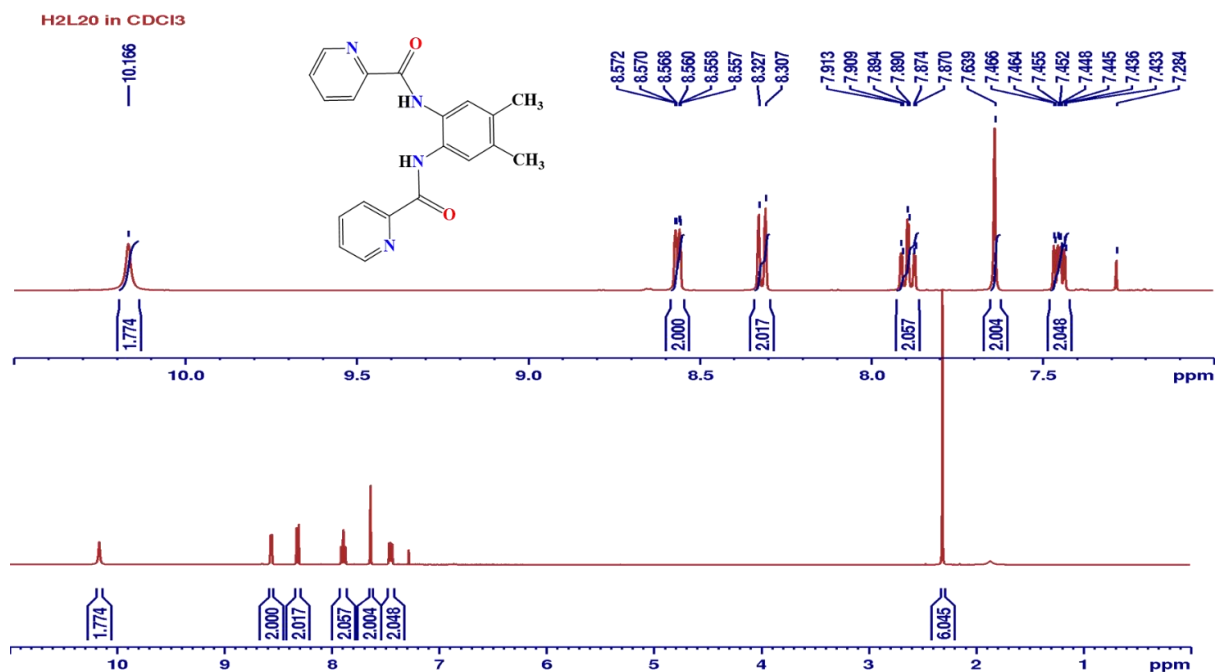


Figure S2. ¹H NMR spectrum of *N,N'*-(4,5-dimethyl-1,2-phenylene)dipicolinamide: **H₂L2** showing N-H signal at 10.17 ppm.

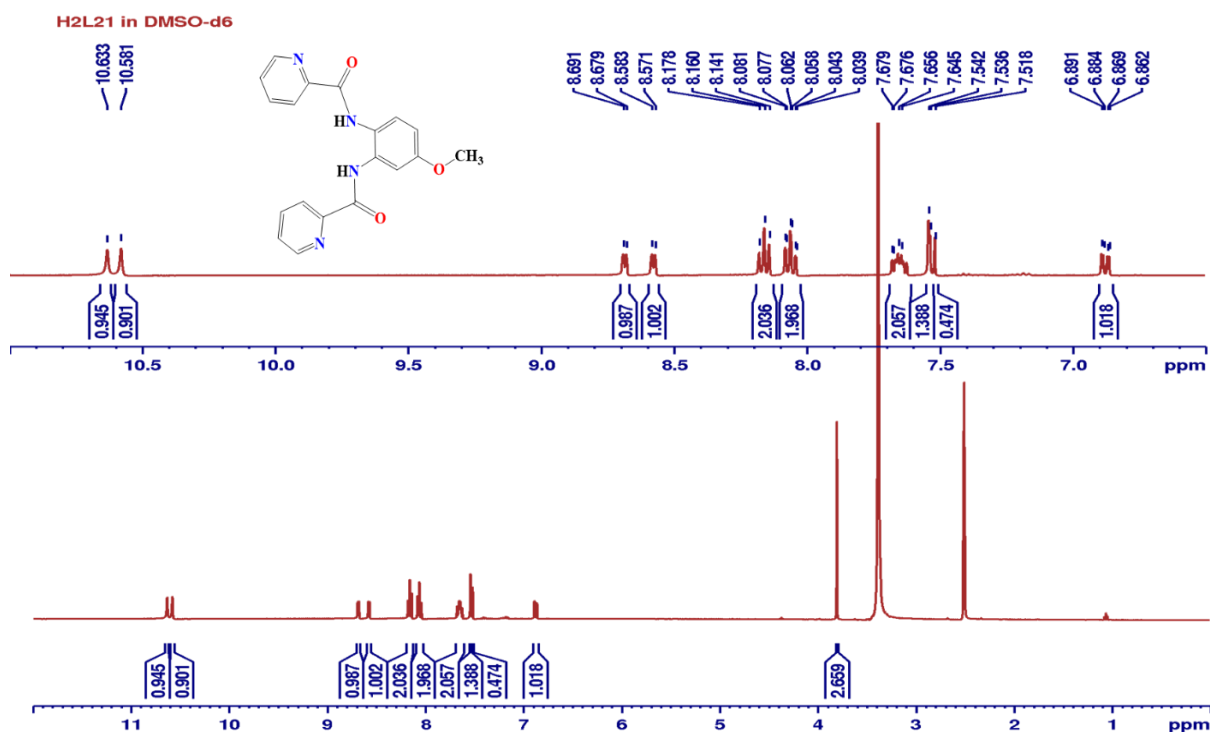


Figure S3. ¹H NMR spectrum of *N,N'*-(3-methoxy-1,2-phenylene)dipicolinamide: **H₂L3** showing N-H signal at 10.63 and 10.58 ppm.

Ru2L1 in DMSO-d6

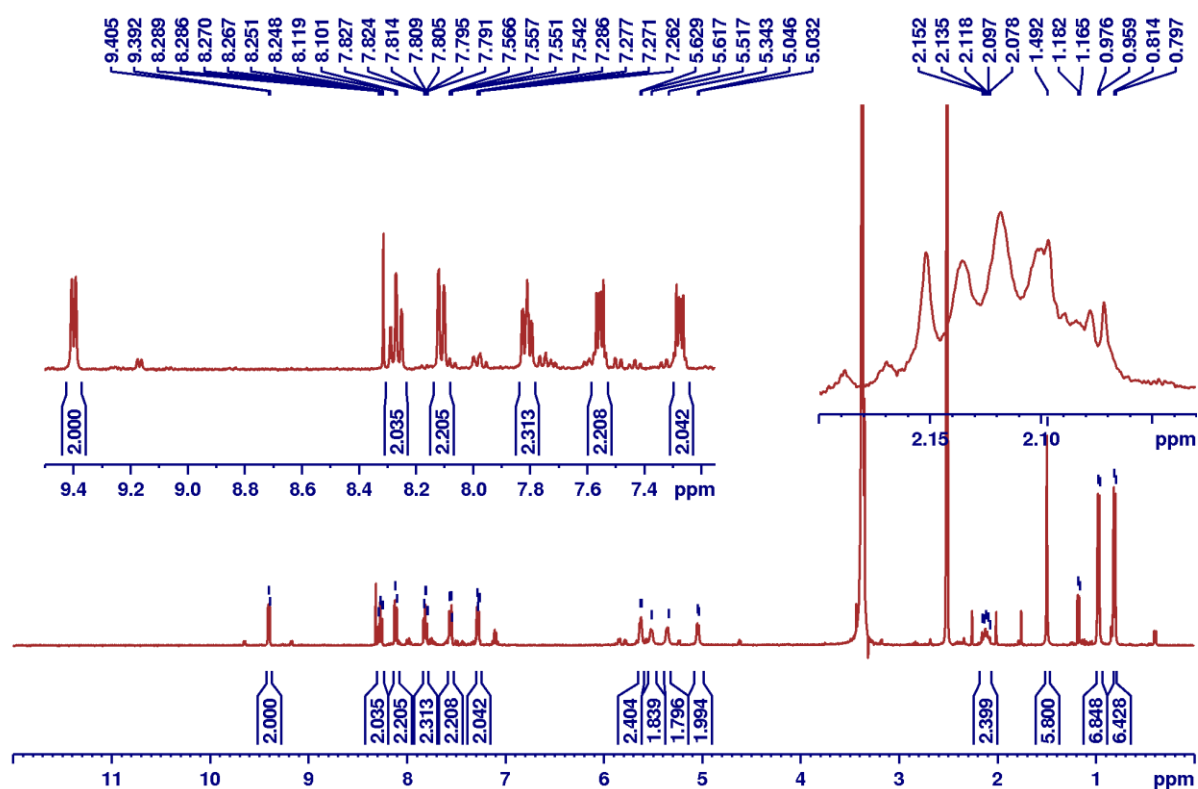


Figure S4. ^1H NMR spectrum of complex **Ru1**.

Ru2L11 (B) in DMSO-d6

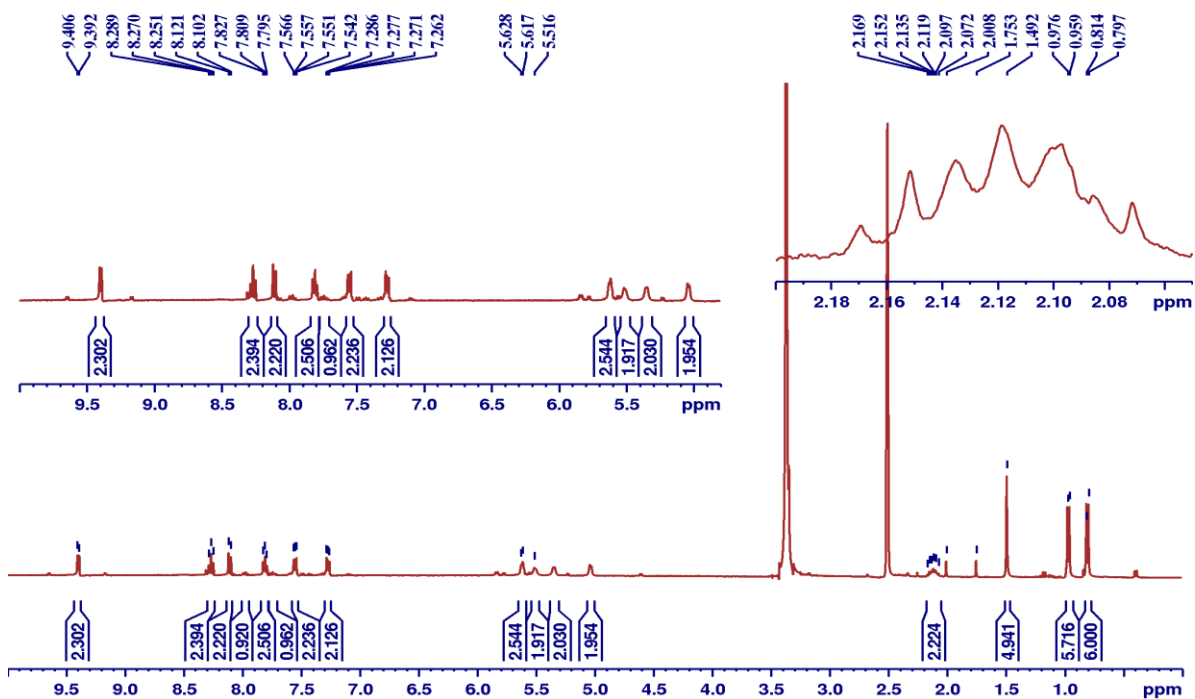


Figure S5. ^1H NMR spectrum of complex **Ru2**.

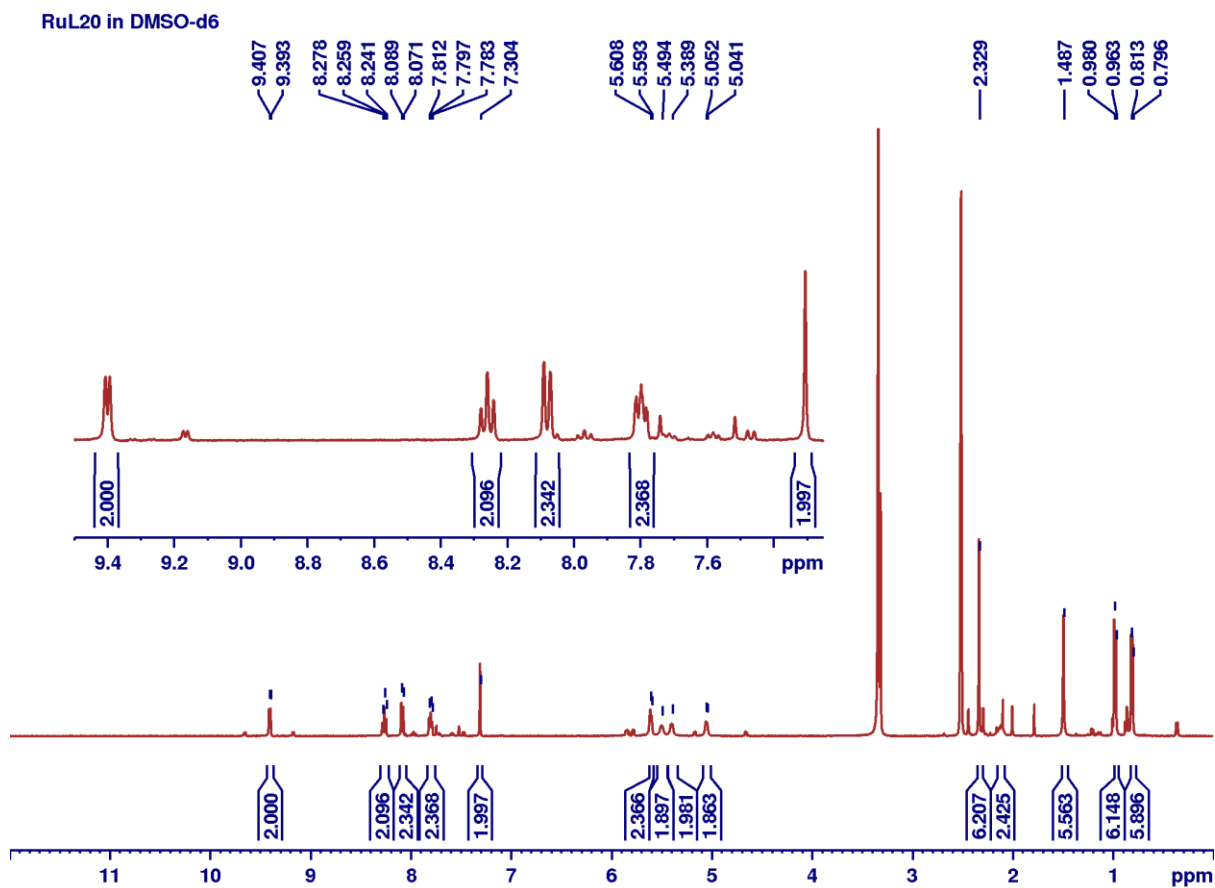


Figure S6. ¹H NMR spectrum of complex **Ru3**.

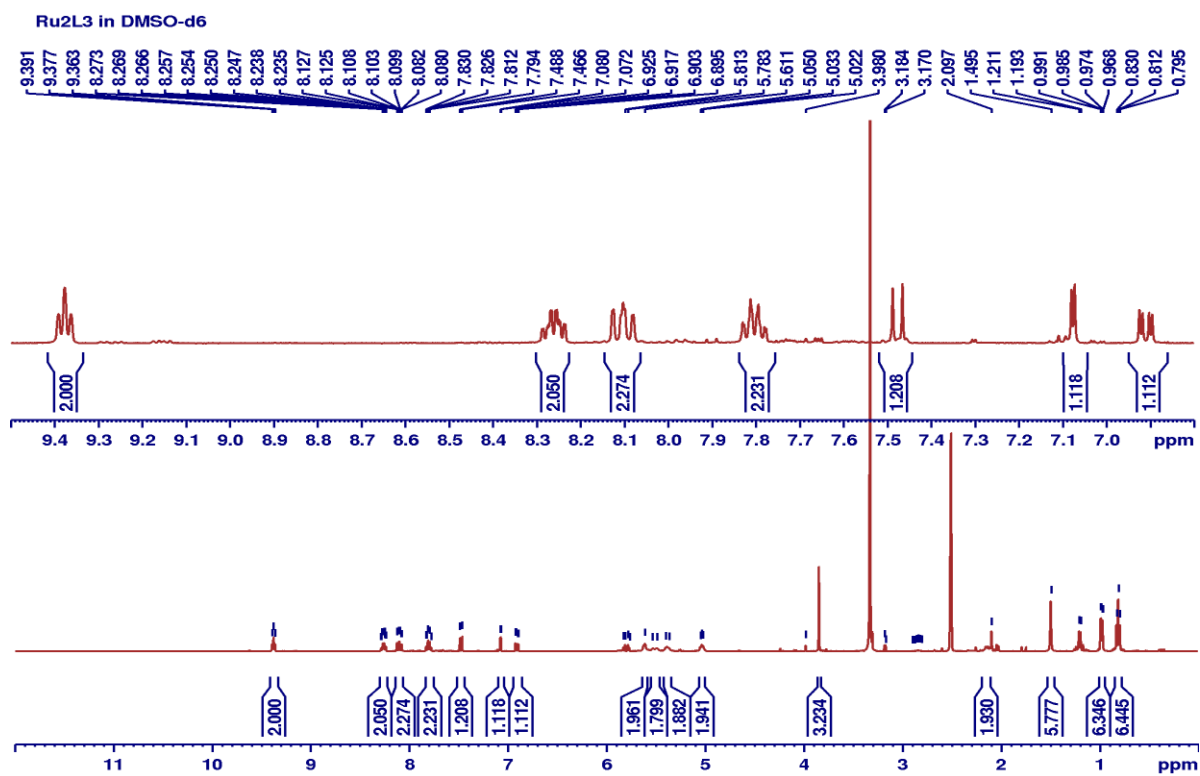


Figure S7. ¹H NMR spectrum of complex **Ru4**.

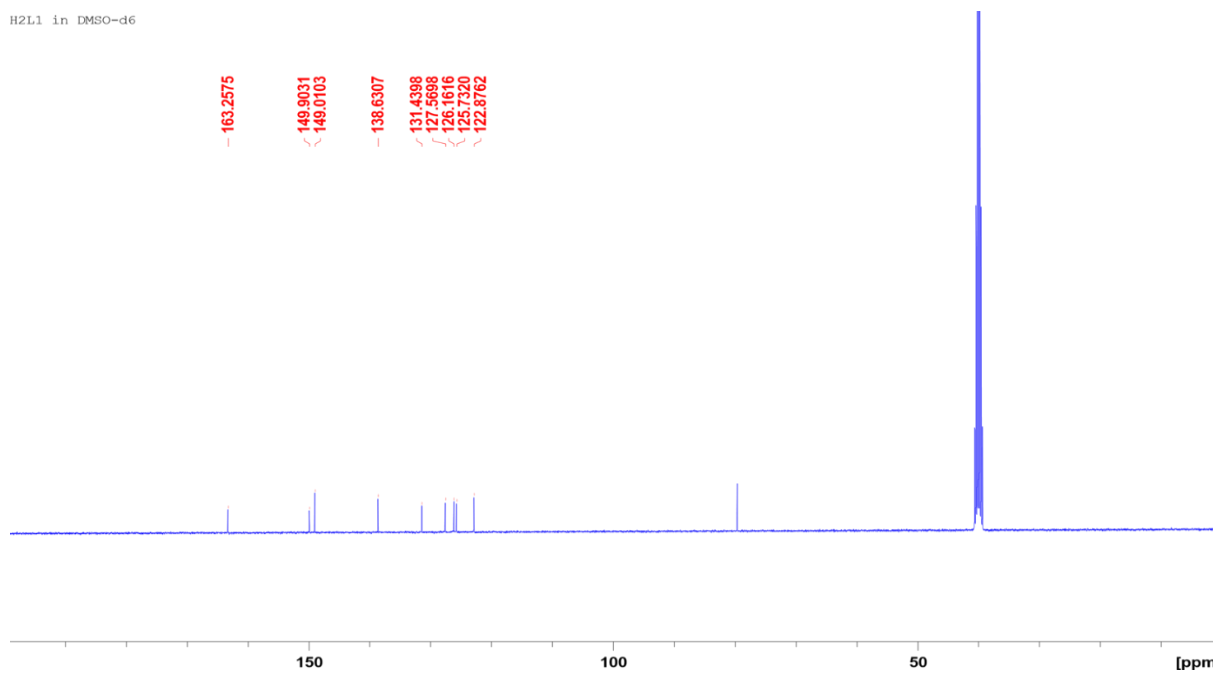


Figure S8. $^{13}\text{C}\{^1\text{H}\}$ NMR spectrum of *N,N'*-(1,2-phenylene)dipicolinamide: **H₂L1**.

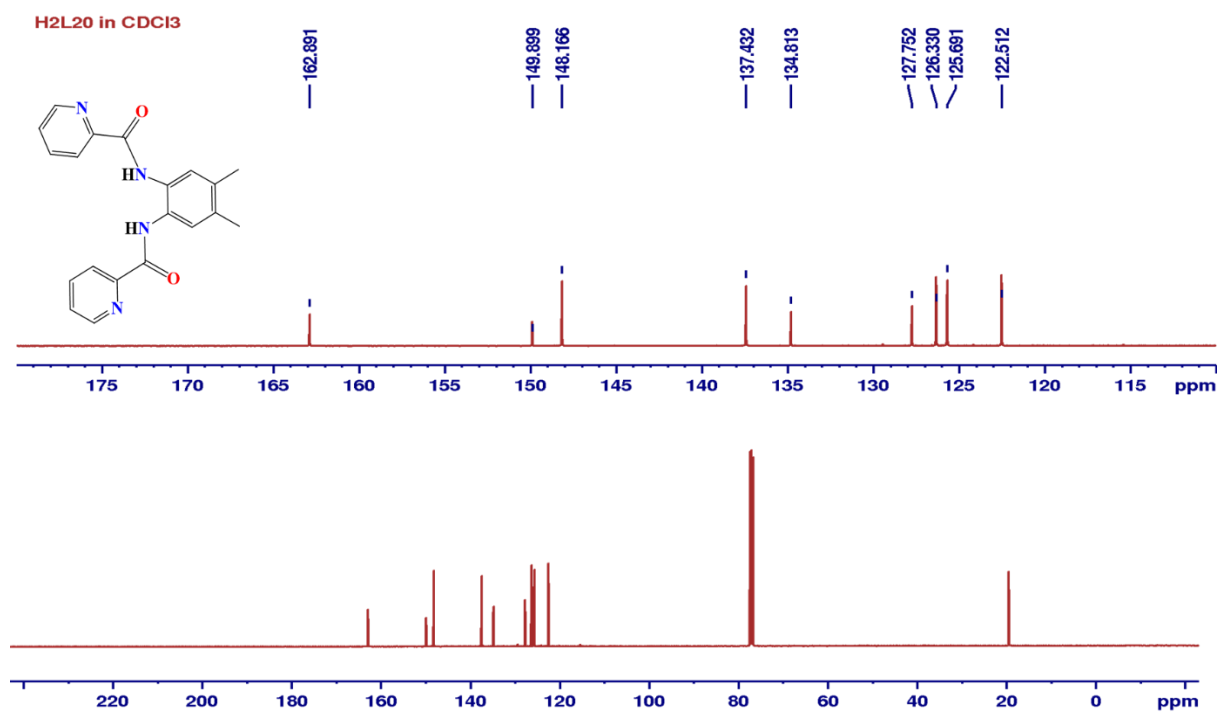


Figure S9. $^{13}\text{C}\{^1\text{H}\}$ NMR spectrum of *N,N'*-(4,5-dimethyl-1,2-phenylene)dipicolinamide: **H₂L2**.

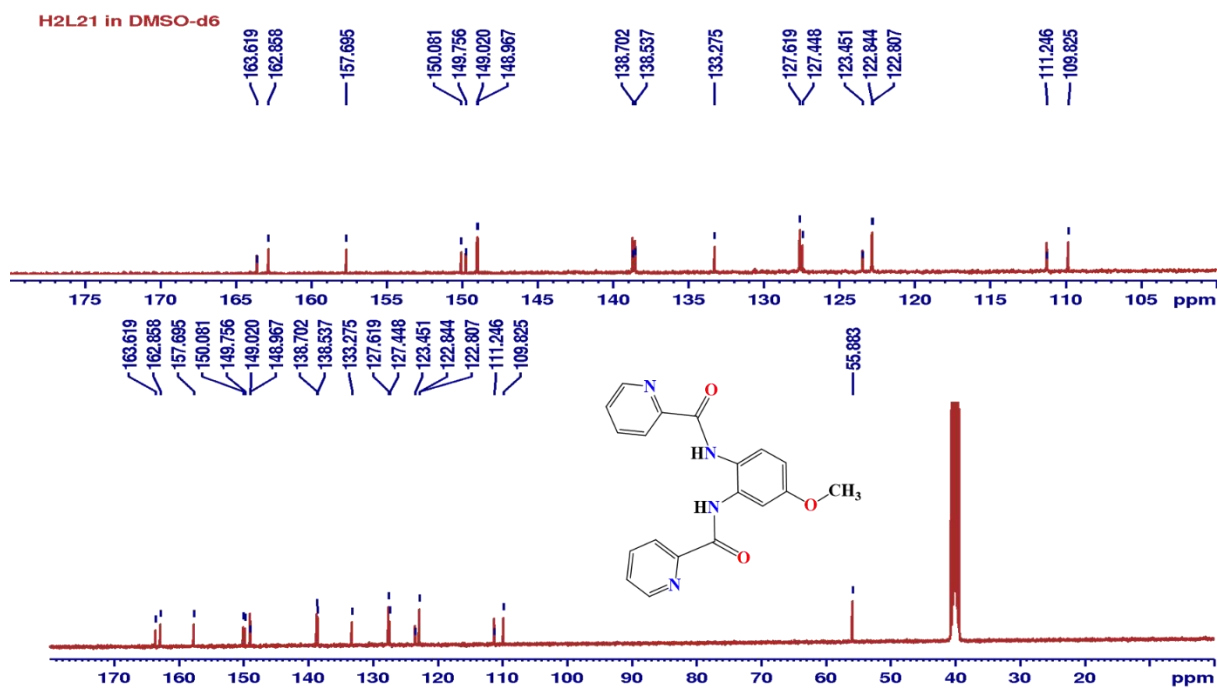


Figure S10. $^{13}\text{C}\{^1\text{H}\}$ NMR spectrum of *N,N'*-(3-methoxy-1,2-phenylene)dipicolinamide: **H2L3**.

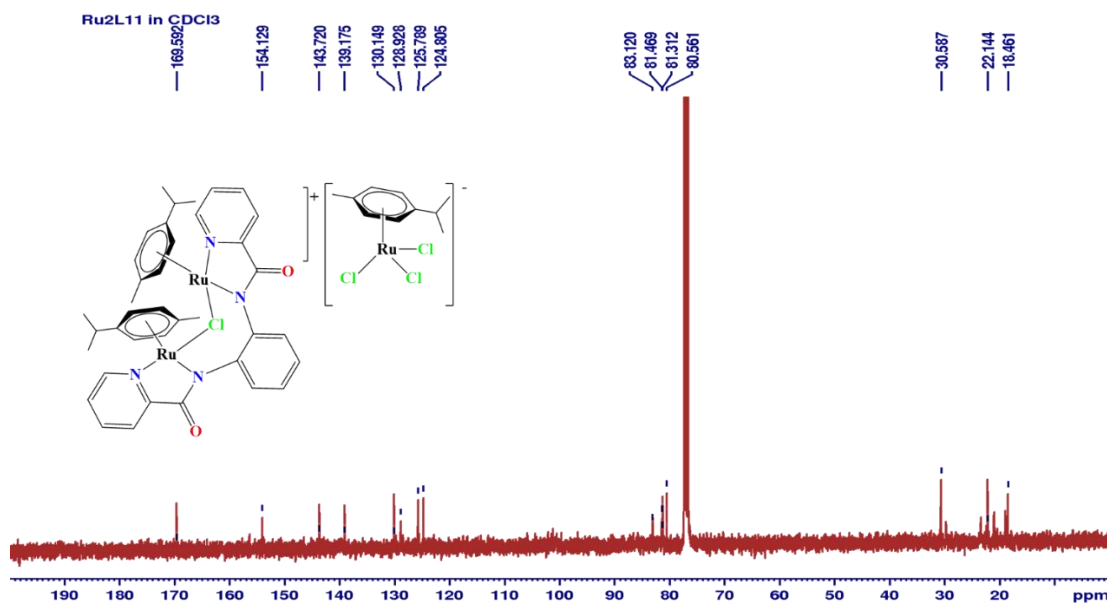


Figure S11. ^{13}C NMR spectrum of complex **Ru1**.

Ru2L11(b) in CDCl₃

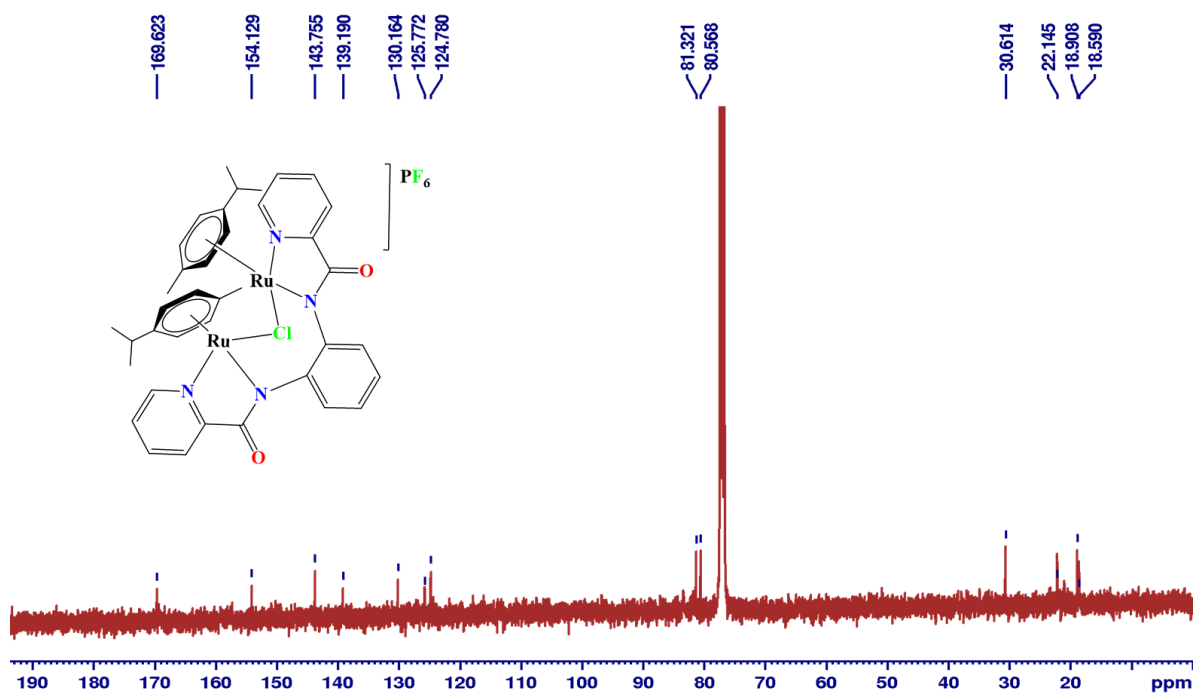


Figure S12. ¹³C NMR spectrum of complex Ru2.

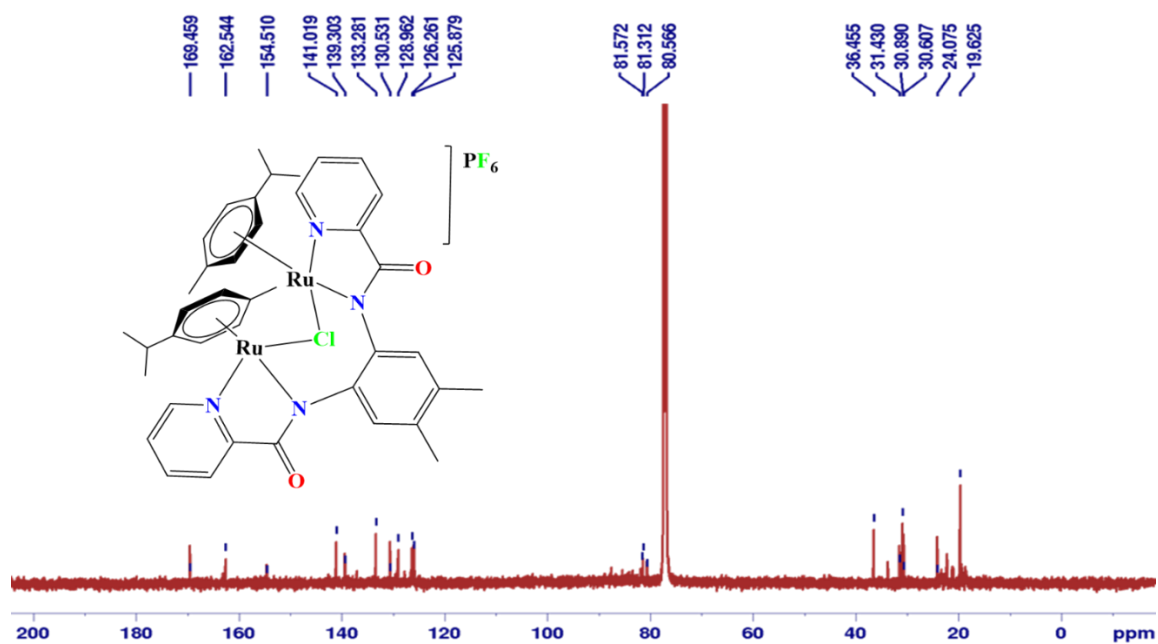


Figure S13. ¹³C NMR spectrum of complex Ru3.

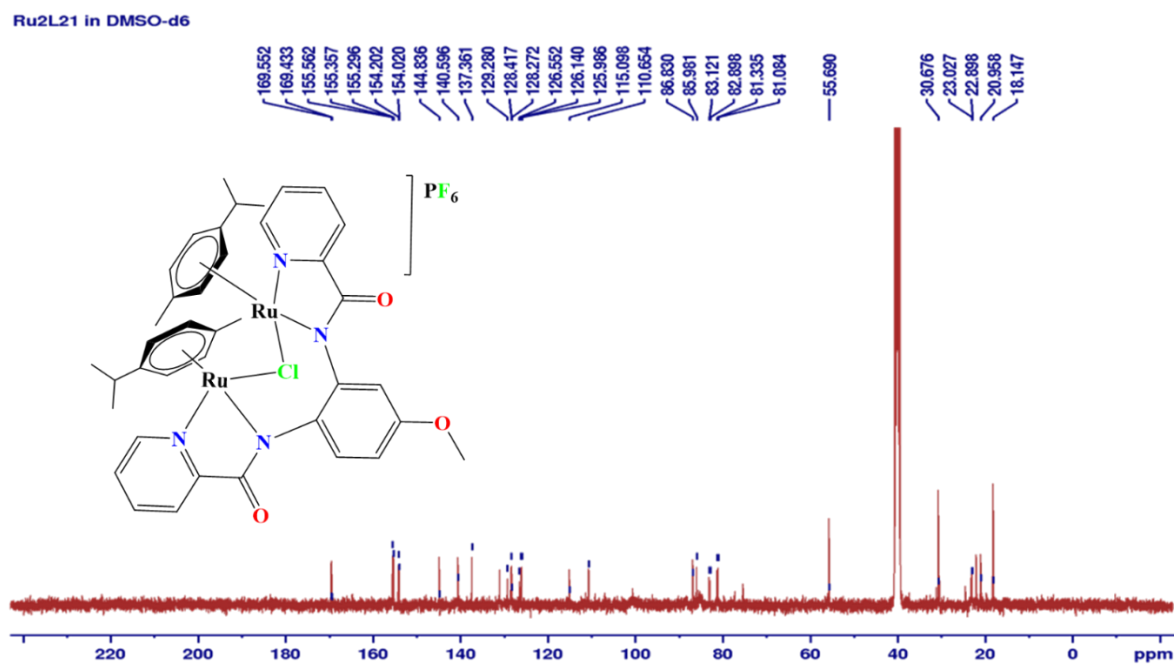


Figure S14. ^{13}C NMR spectrum of complex **Ru4**.

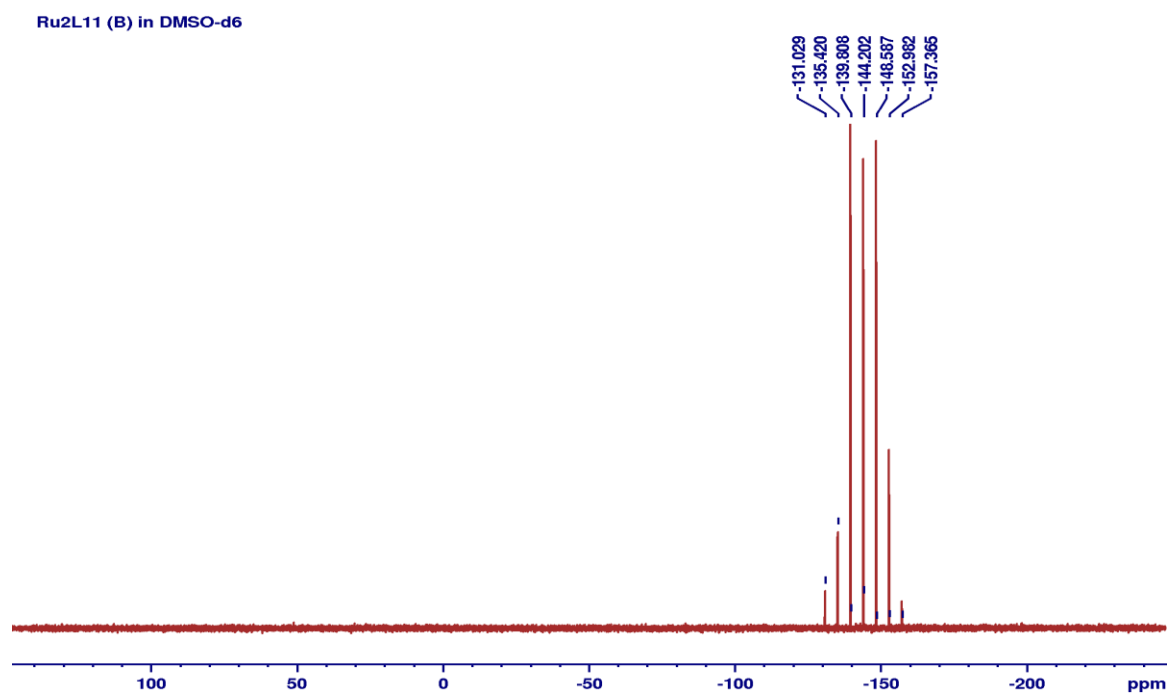


Figure S15. ^{31}P NMR of complex **Ru2** at room temperature.

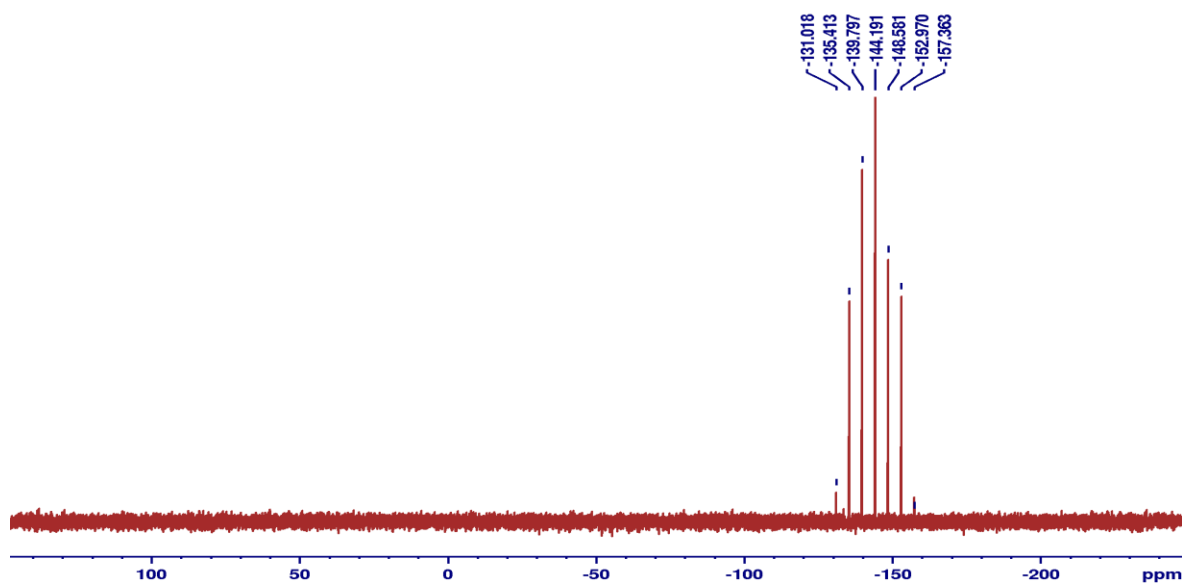


Figure S16. ^{31}P NMR of complex **Ru3** at room temperature.

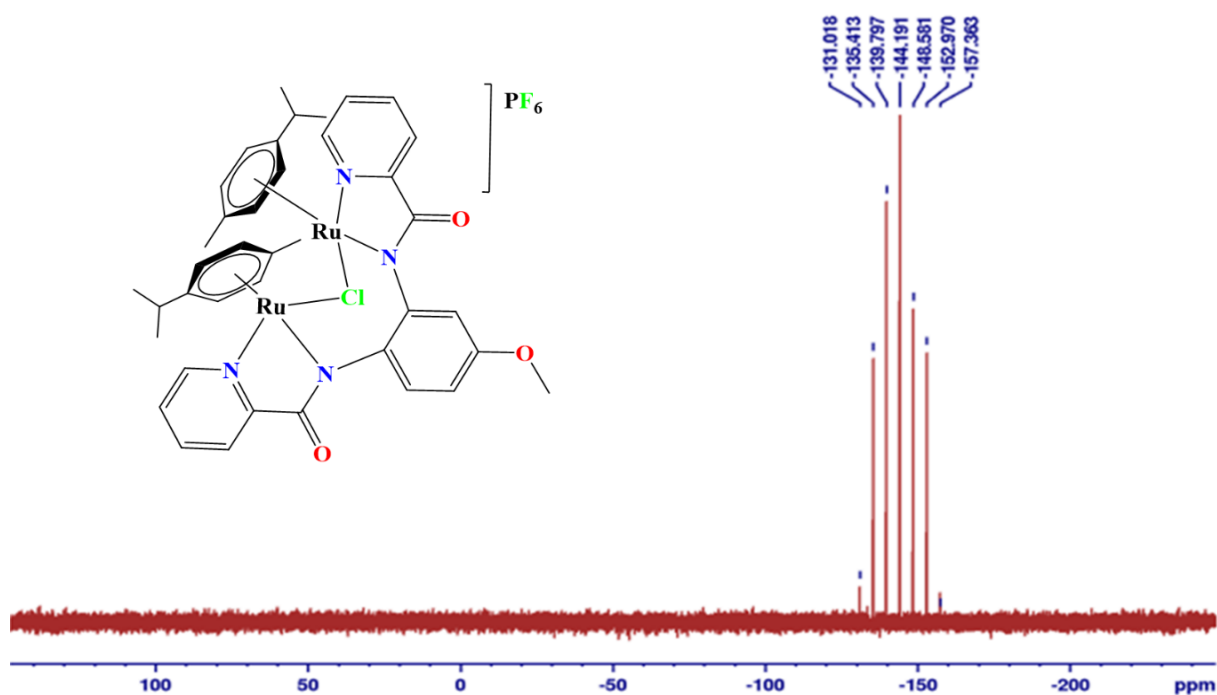


Figure S17. ^{31}P NMR of complex **Ru4** at room temperature.

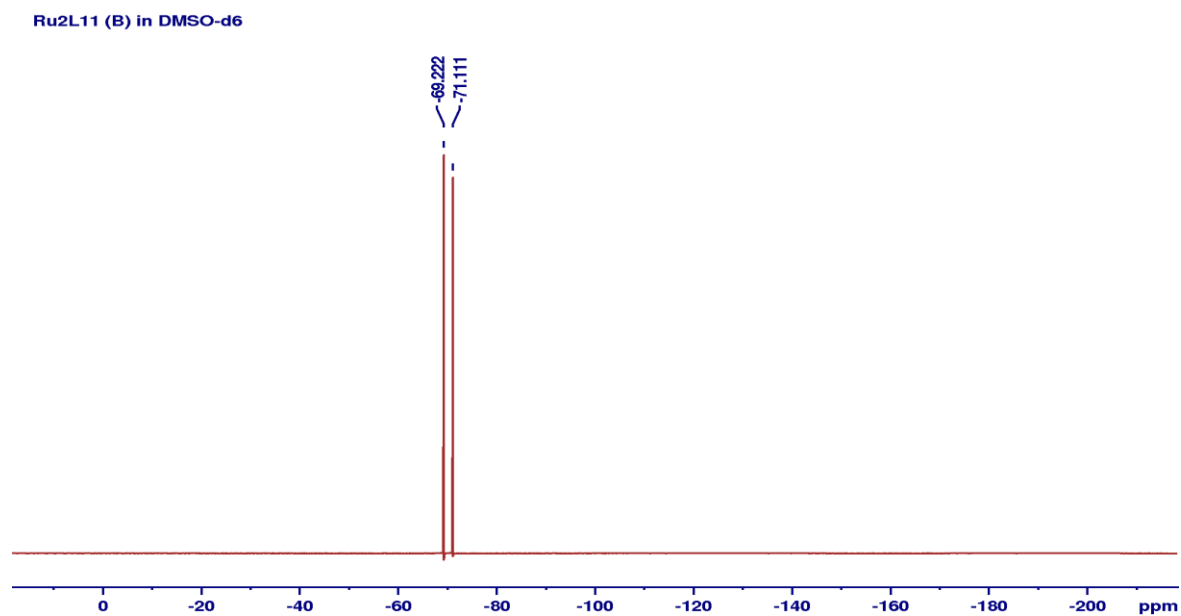


Figure S18. ^{19}F NMR of complex **Ru2** at room temperature.

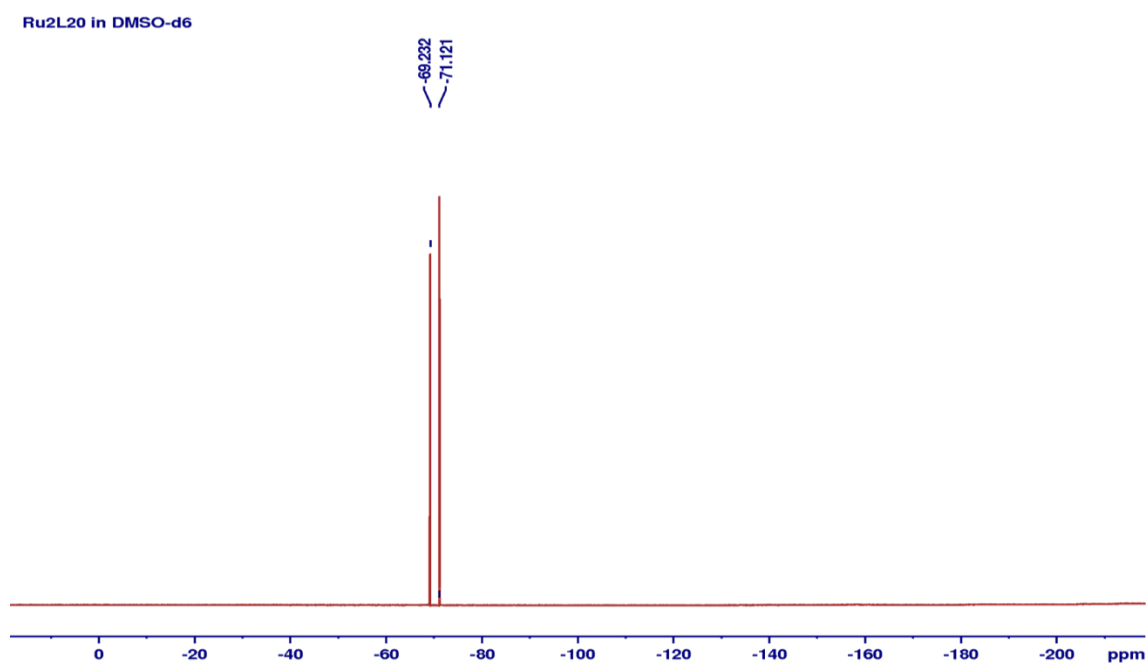


Figure S19. ^{19}F NMR of complex **Ru3** at room temperature.

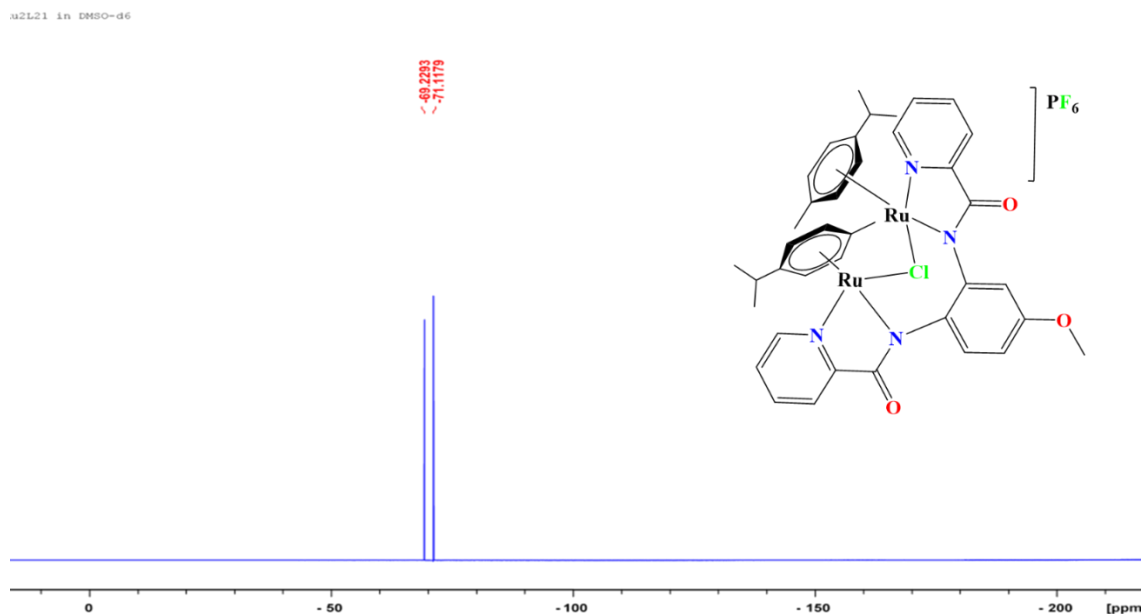


Figure S20. ^{19}F NMR of complex **Ru4** in d_6 -DMSO at room temperature.

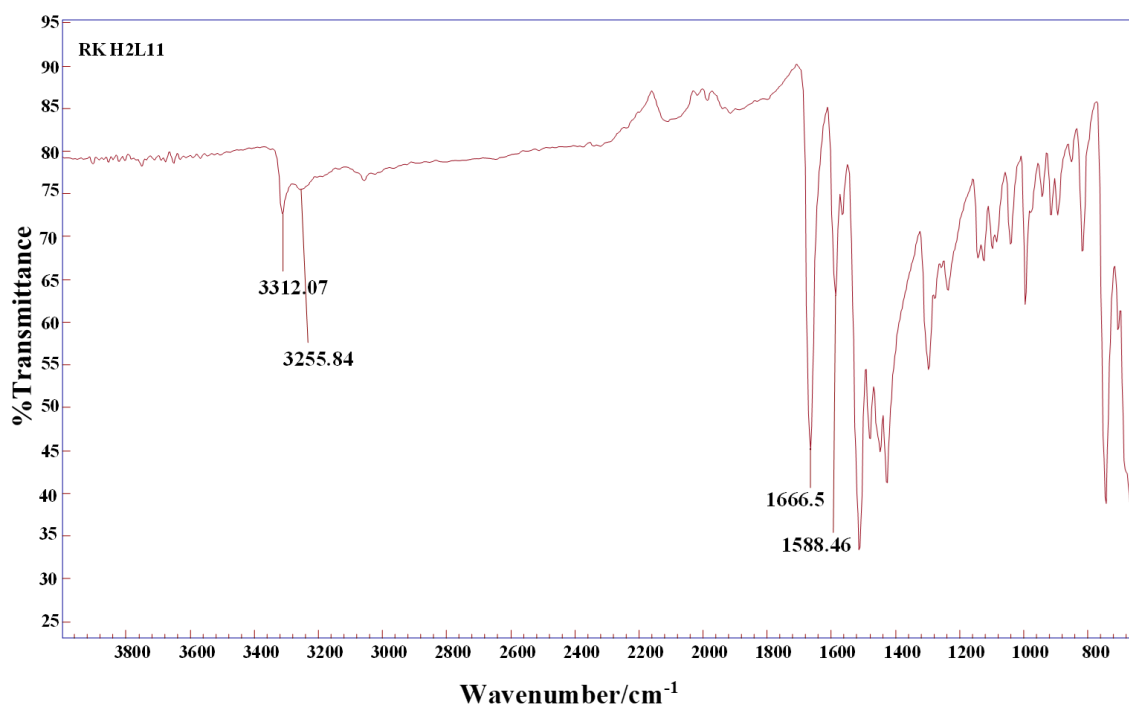


Figure S21. FT-IR of Ligand N,N' -(1,2-phenylene)dipicolinamide **H₂L1** showing the carbonyl peak at 1667 cm^{-1} .

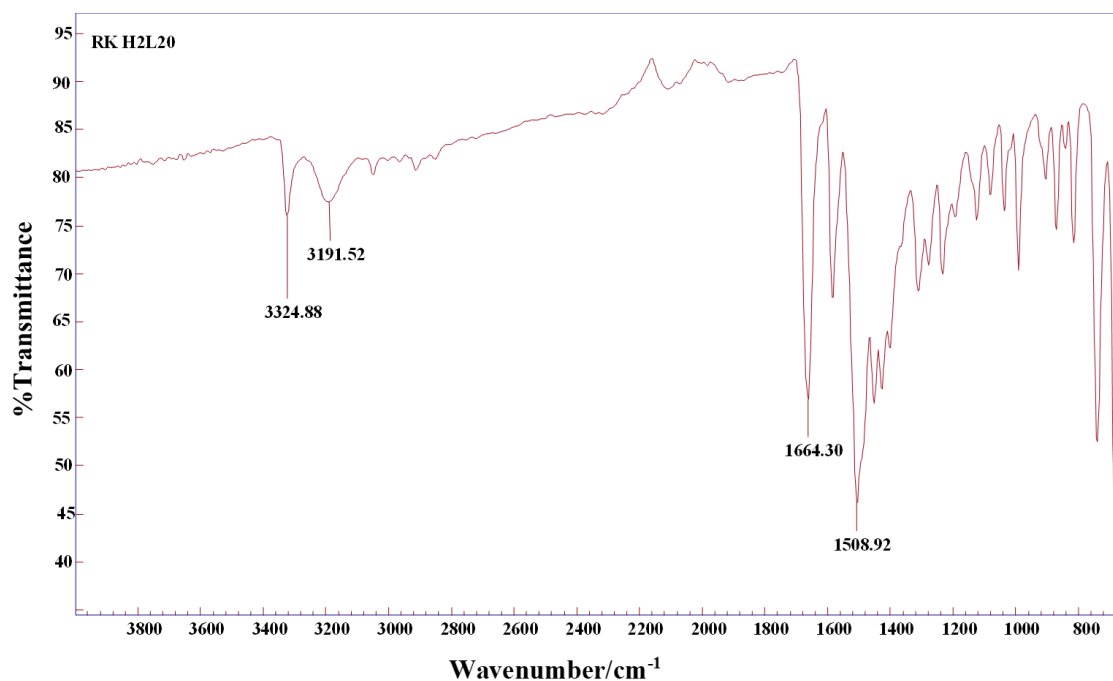


Figure S22. FT-IR of spectrum of *N,N'*-(4,5-dimethyl-1,2-phenylene)dipicolinamide: **H₂L2** showing its carbonyl peak at 1664 cm⁻¹.

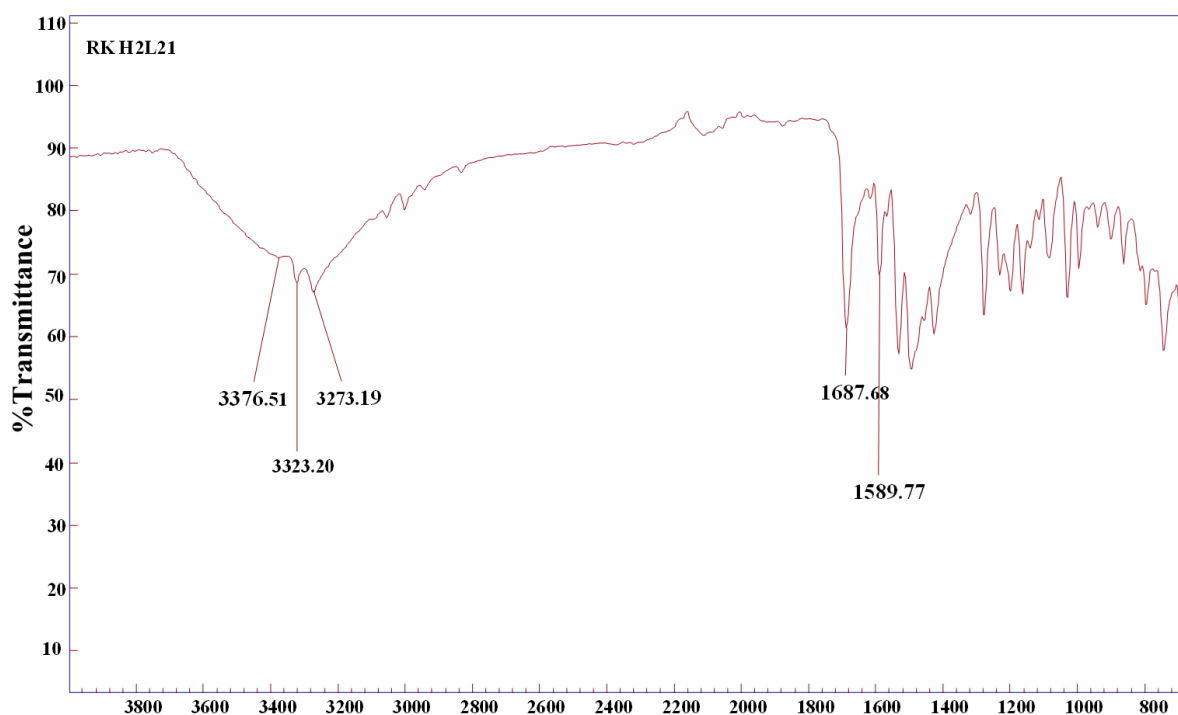


Figure S23. FT-IR of spectrum of *N,N'*-(3-methoxy-1,2-phenylene)dipicolinamide: **H₂L3** showing its carbonyl peak at 1688 cm⁻¹.

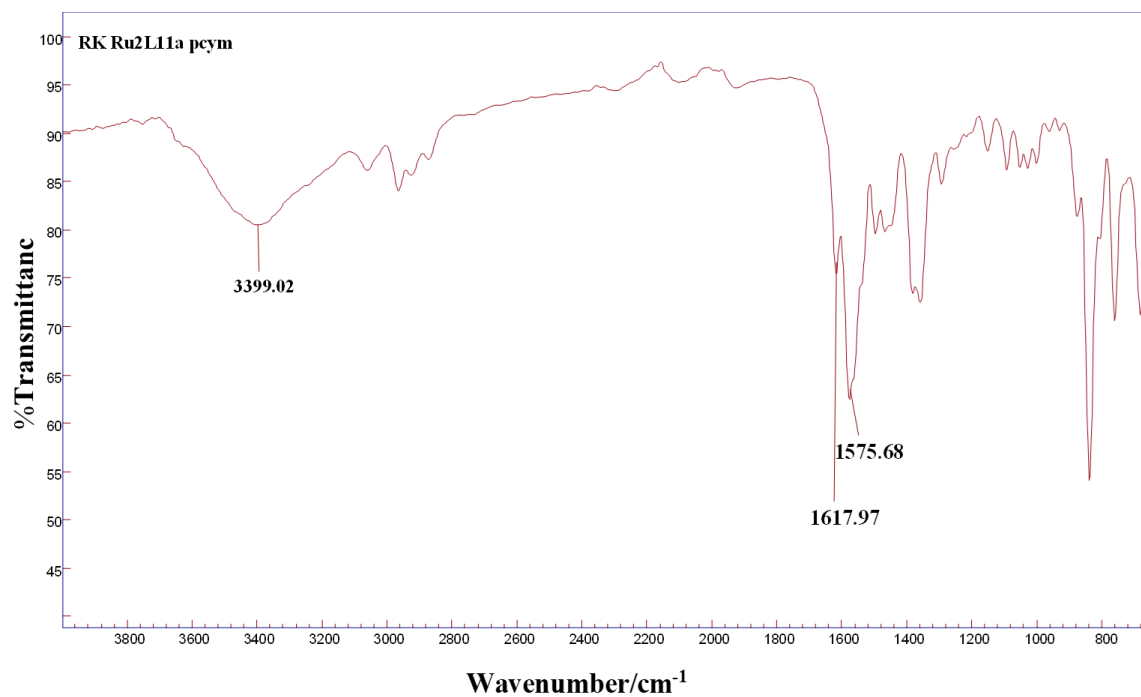


Figure S24. FT-IR of dinuclear complex **Ru1** showing the carbonyl peak at 1618 cm⁻¹.

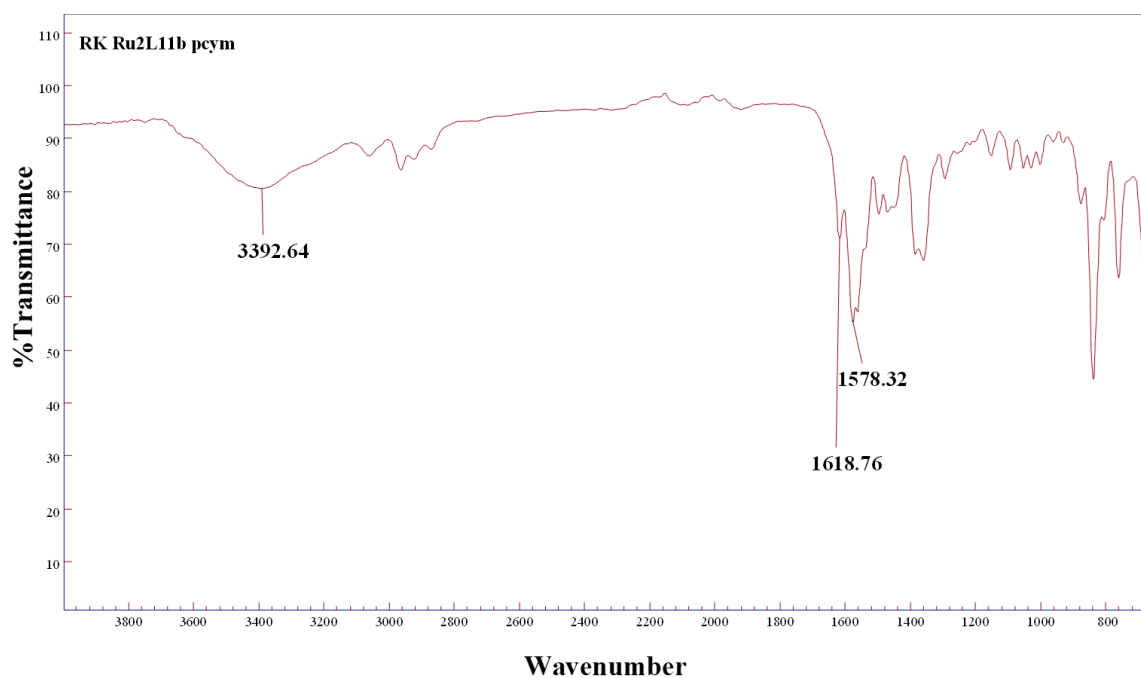


Figure S25. FT-IR of dinuclear complex **Ru2** showing the carbonyl peak at 1619 cm⁻¹.

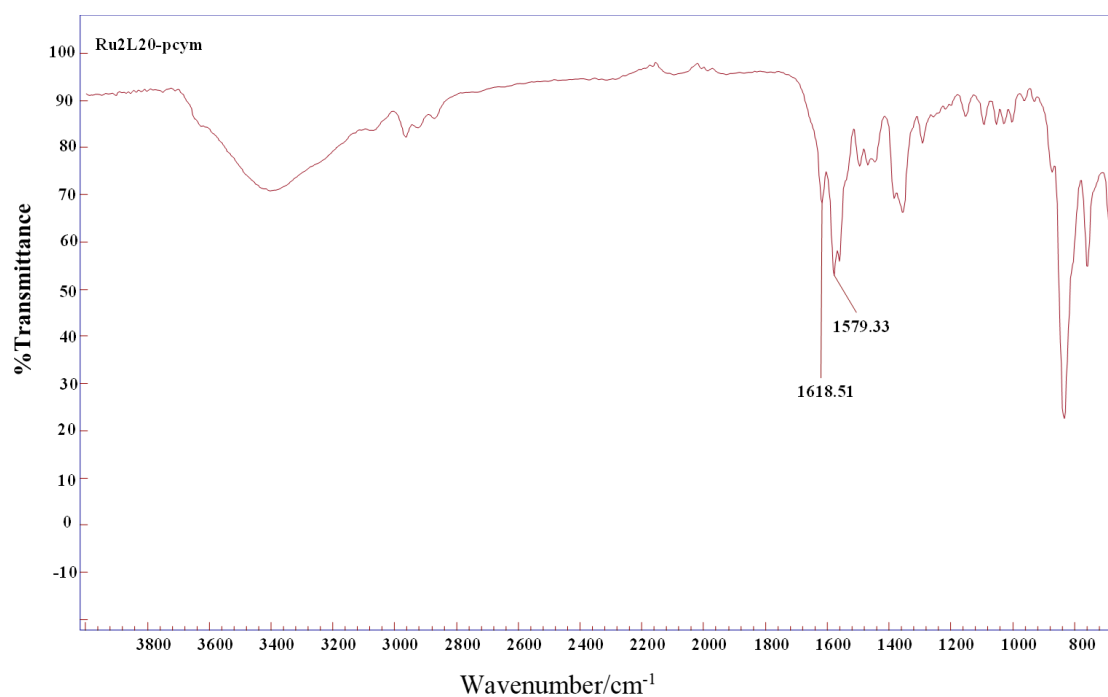


Figure S26. FT-IR of dinuclear complex **Ru3** showing the carbonyl peak at 1619 cm⁻¹.

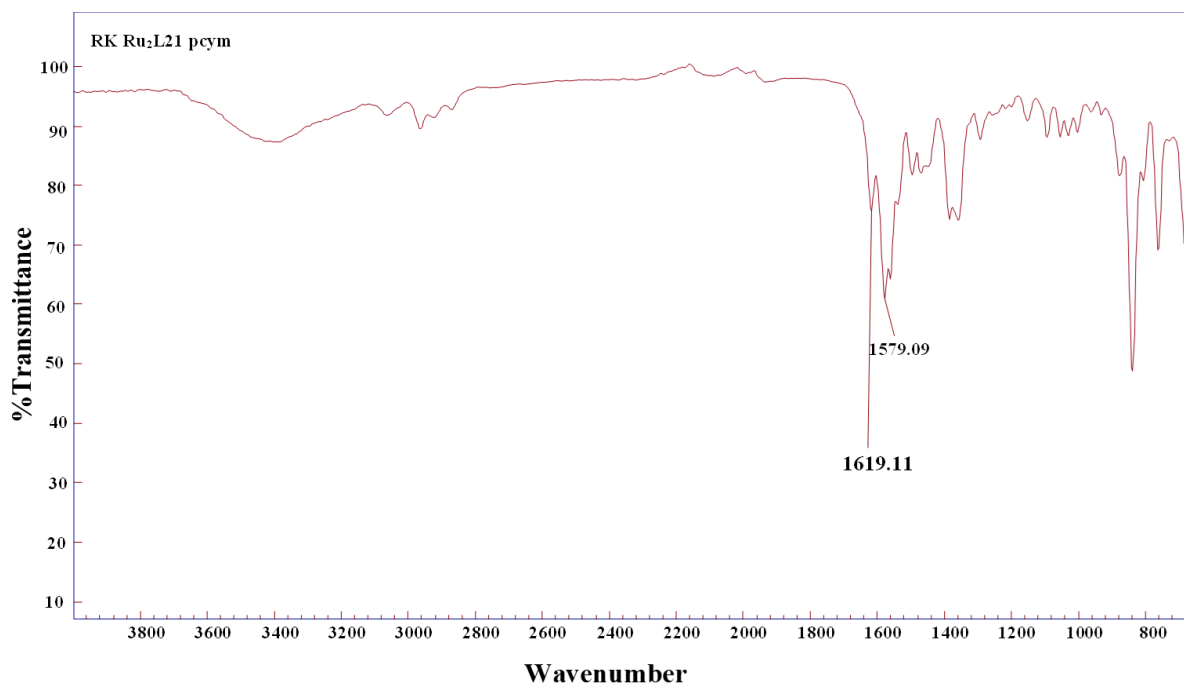


Figure S27. FT-IR of dinuclear complex **Ru4** showing the carbonyl peak at 1619 cm⁻¹.

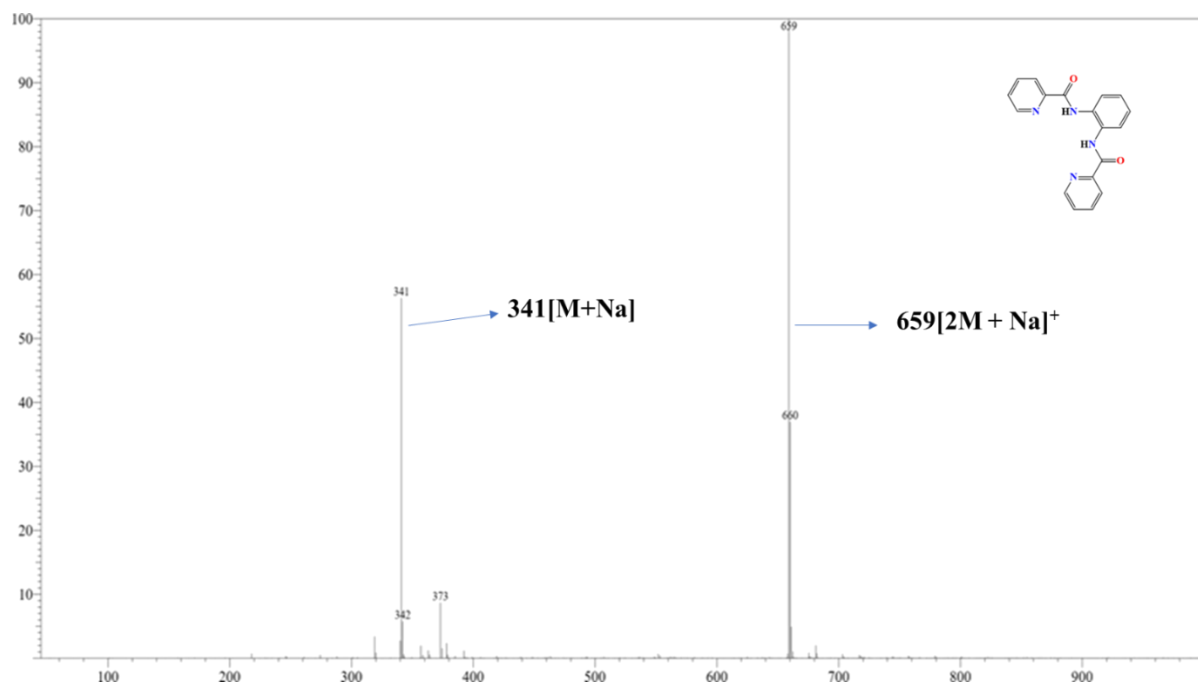


Figure S28. ESI LC-MS (positive mode) of *N,N'*-(1,2-phenylene)bis(pyridine-2-carboxamide): **H₂L1**.

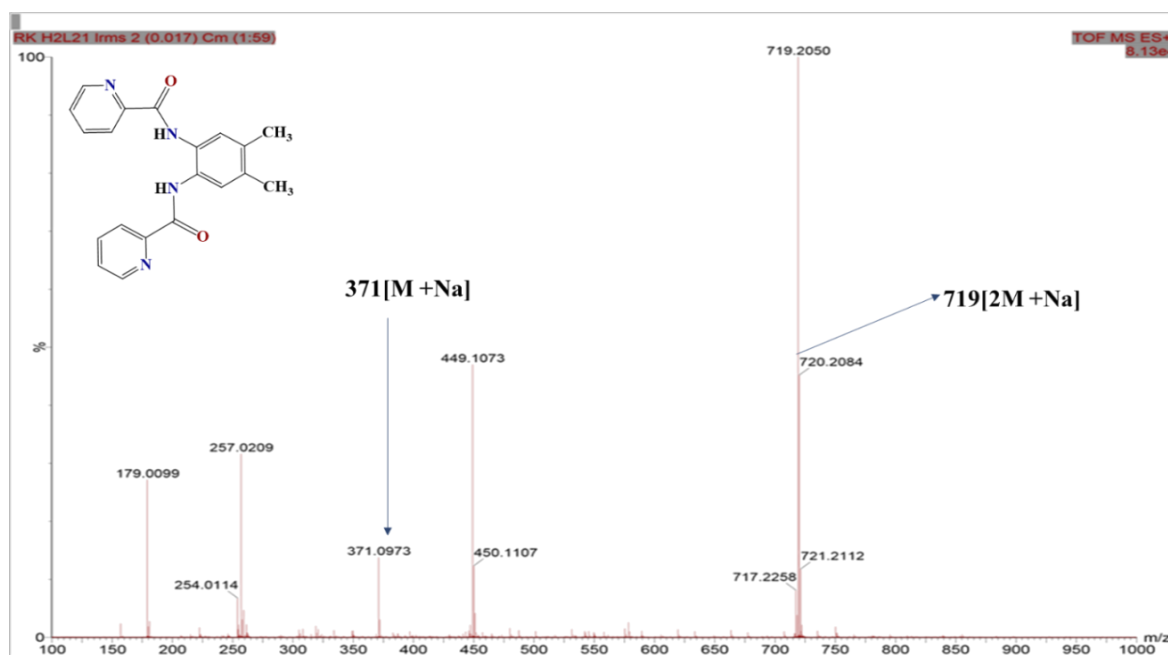


Figure S29. ESI LC-MS (positive mode) of *N,N'*-(4,5-dimethyl-1,2-phenylene)dipicolinamide: **H₂L2**.

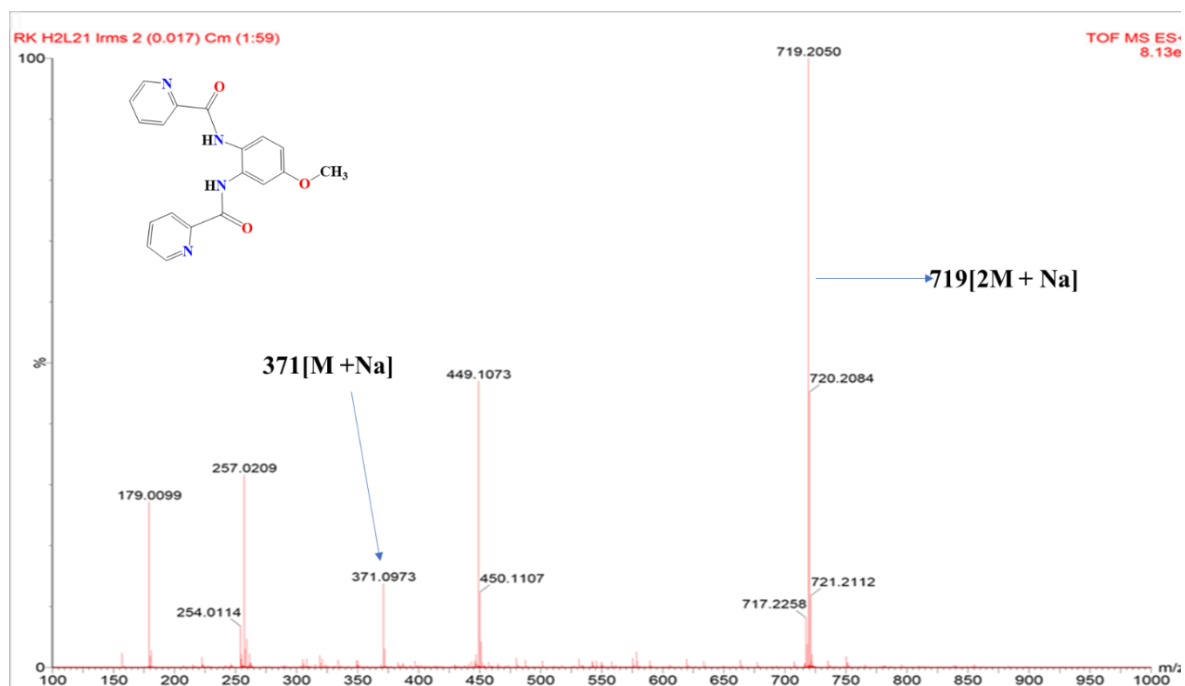


Figure S30. ESI LC-MS (positive mode) of *N,N'*-(4-methoxy-1,2-phenylene)dipicolinamide: **H₂L3**.

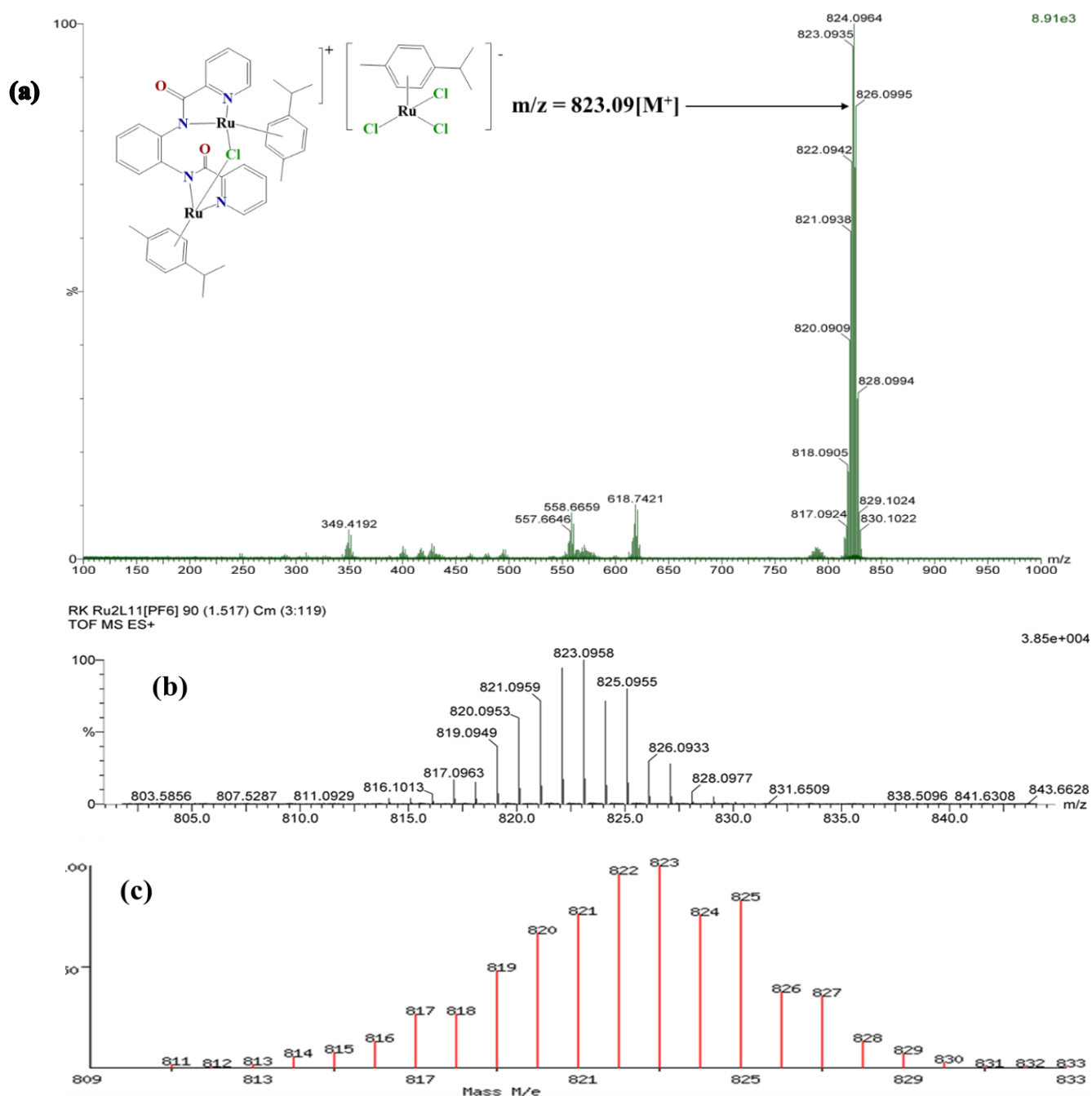


Figure S31. (a) ESI -MS (positive mode) of complex **Ru1**, (b) HR-MS of complex **Ru1**, (c) Theoretical isotopic mass distribution of the complex, **Ru1**.

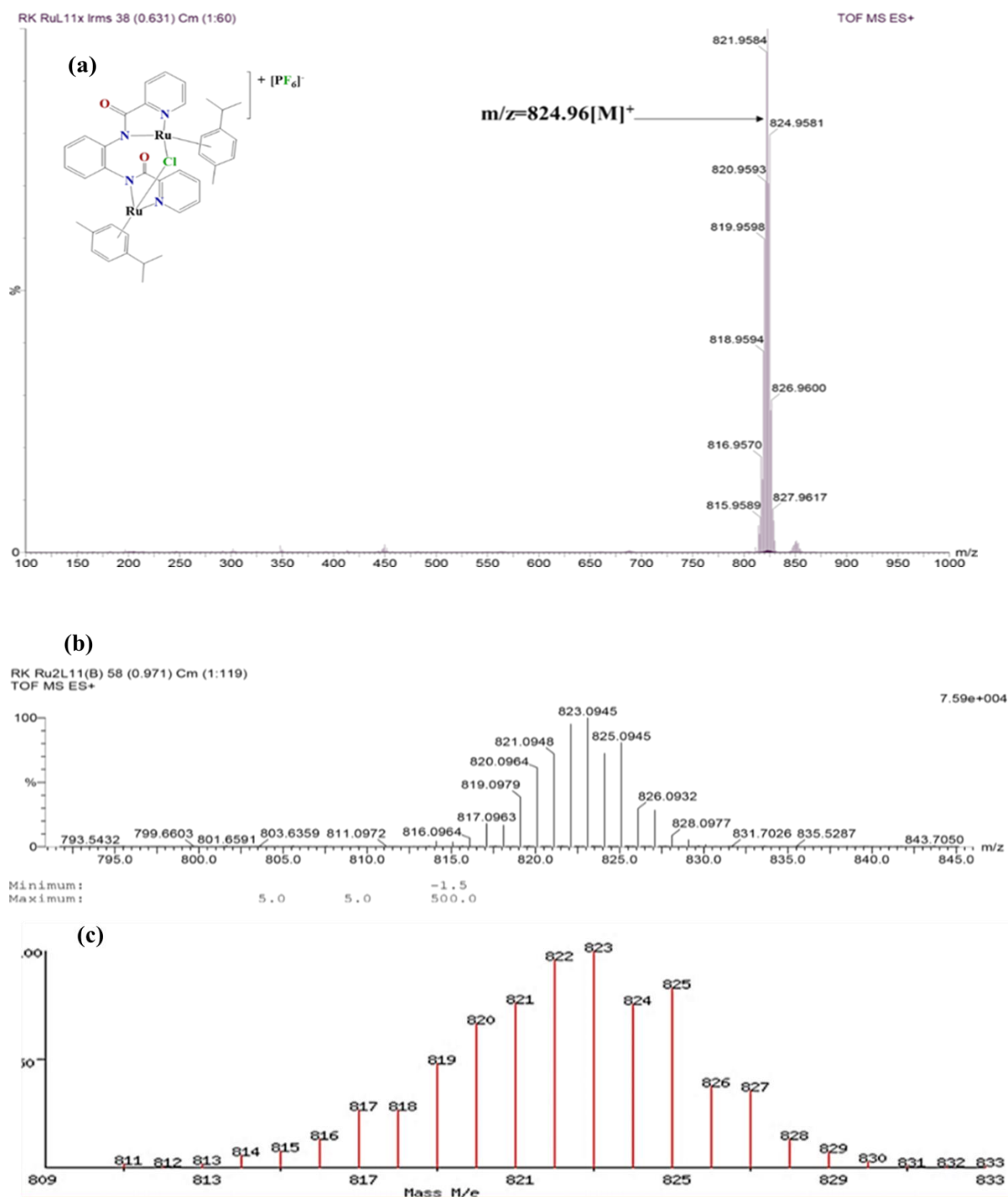


Figure S32. (a) ESI MS of complex **Ru2**, (b) ESI HR-MS of complex **Ru2**, with the molecular formula, (c) Theoretical isotopic mass distribution of the complex, **Ru2**.

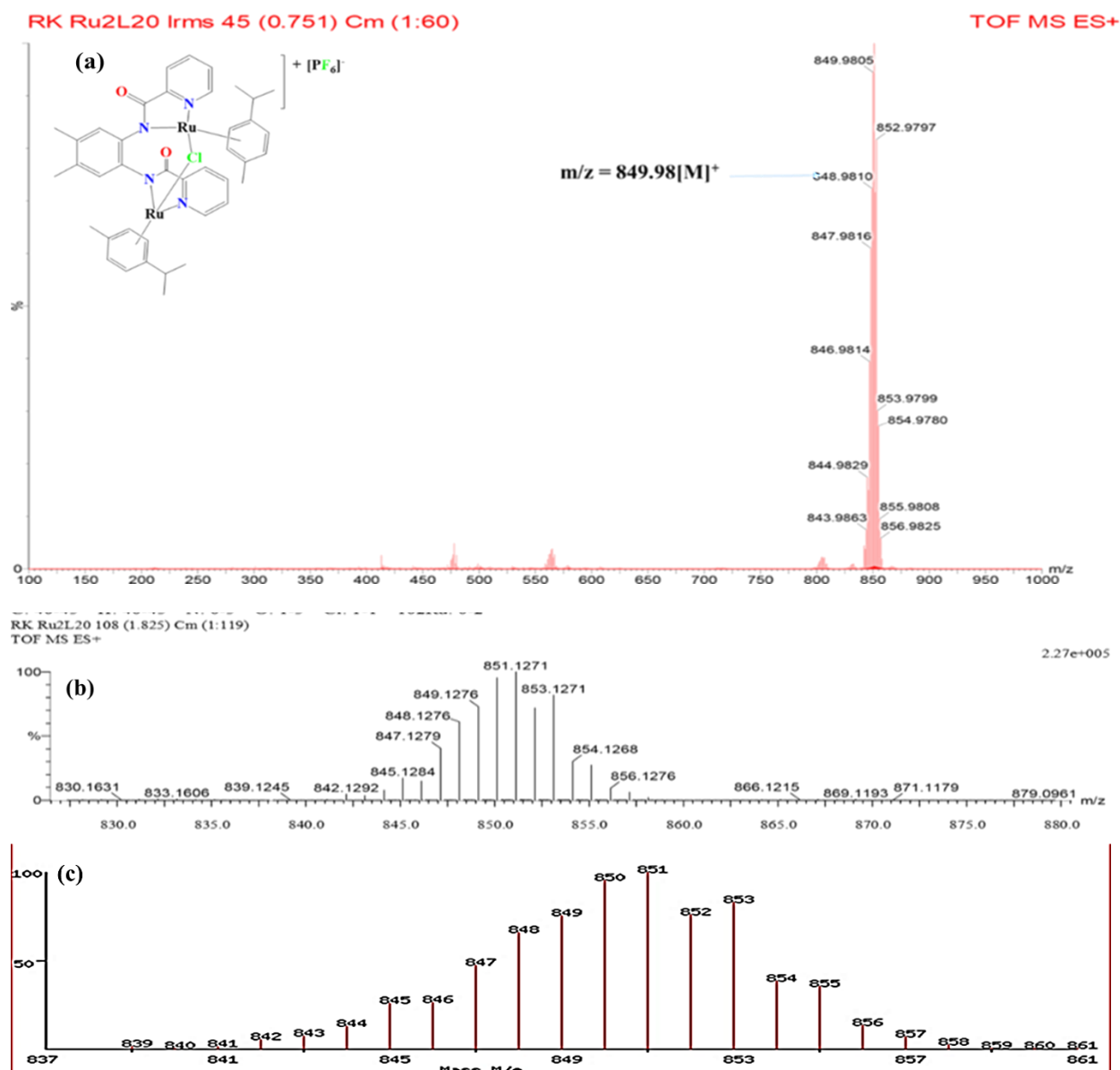


Figure S33. (a) ESI-MS (positive mode) of complex **Ru3**, (b) ESI HR-MS of complex **Ru3**, (c) Theoretical isotopic mass distribution of the complex, **Ru3**.

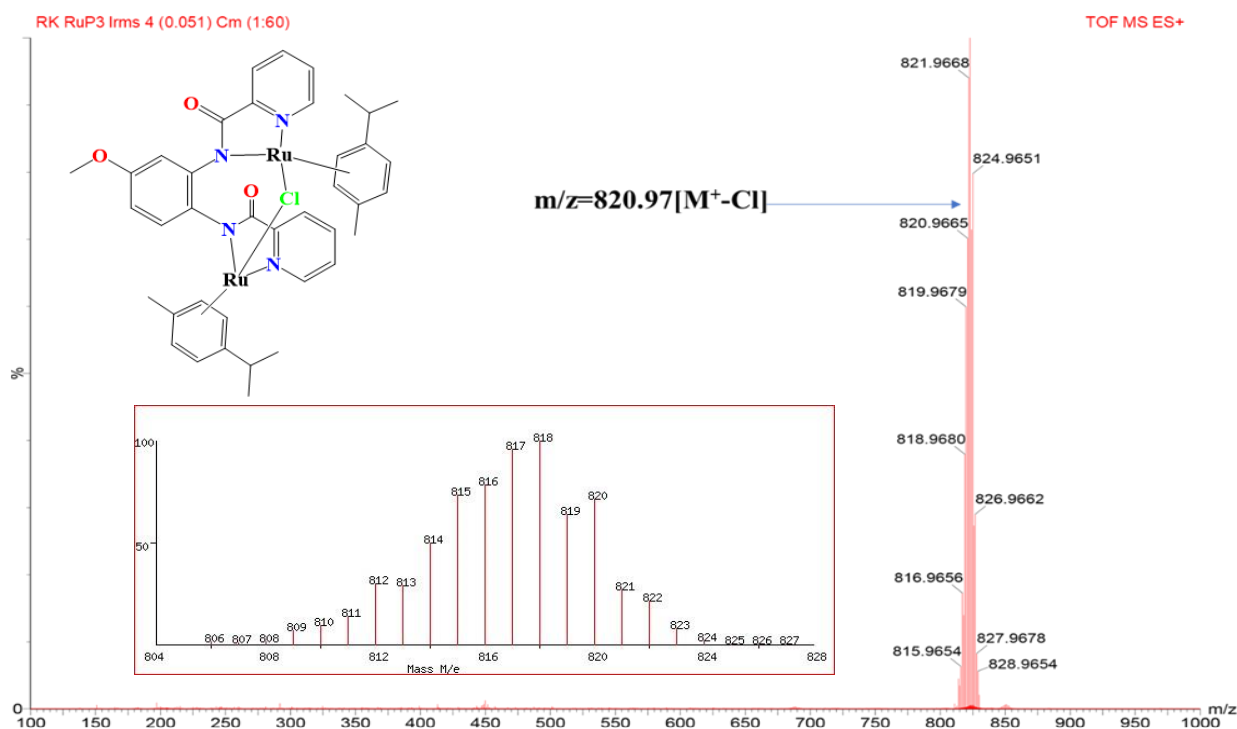


Figure S34. ESI-MS (positive mode) of complex **Ru4**, Theoretical isotopic mass distribution mass spectrometry of **Ru4** (Inset).

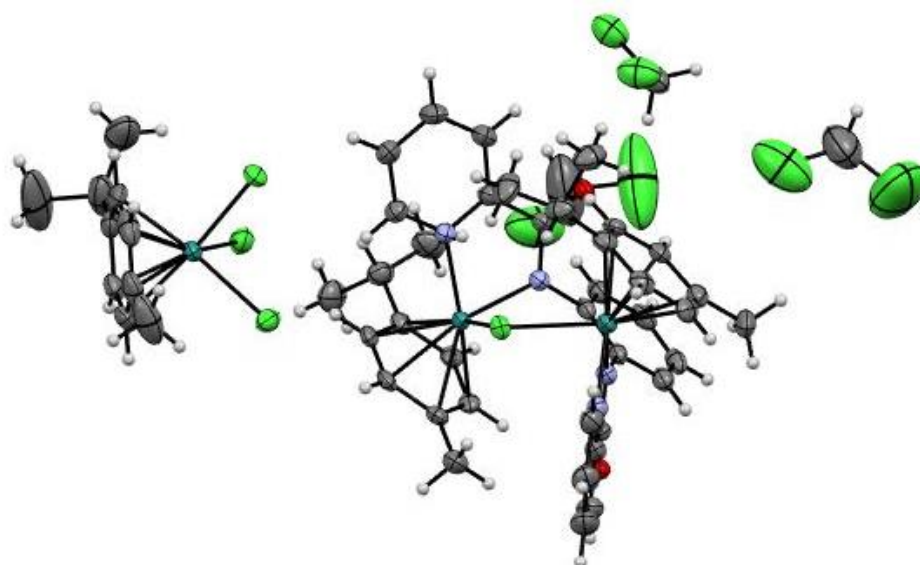


Figure S35. Molecular structure of **Ru1**, with ellipsoids drawn at 50% probability level.

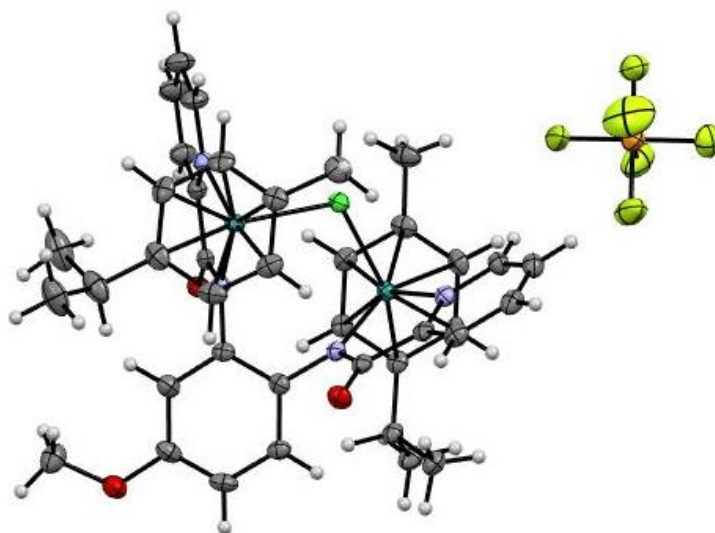


Figure S36. Molecular structure of **Ru4**, with ellipsoids drawn at 50% probability level.

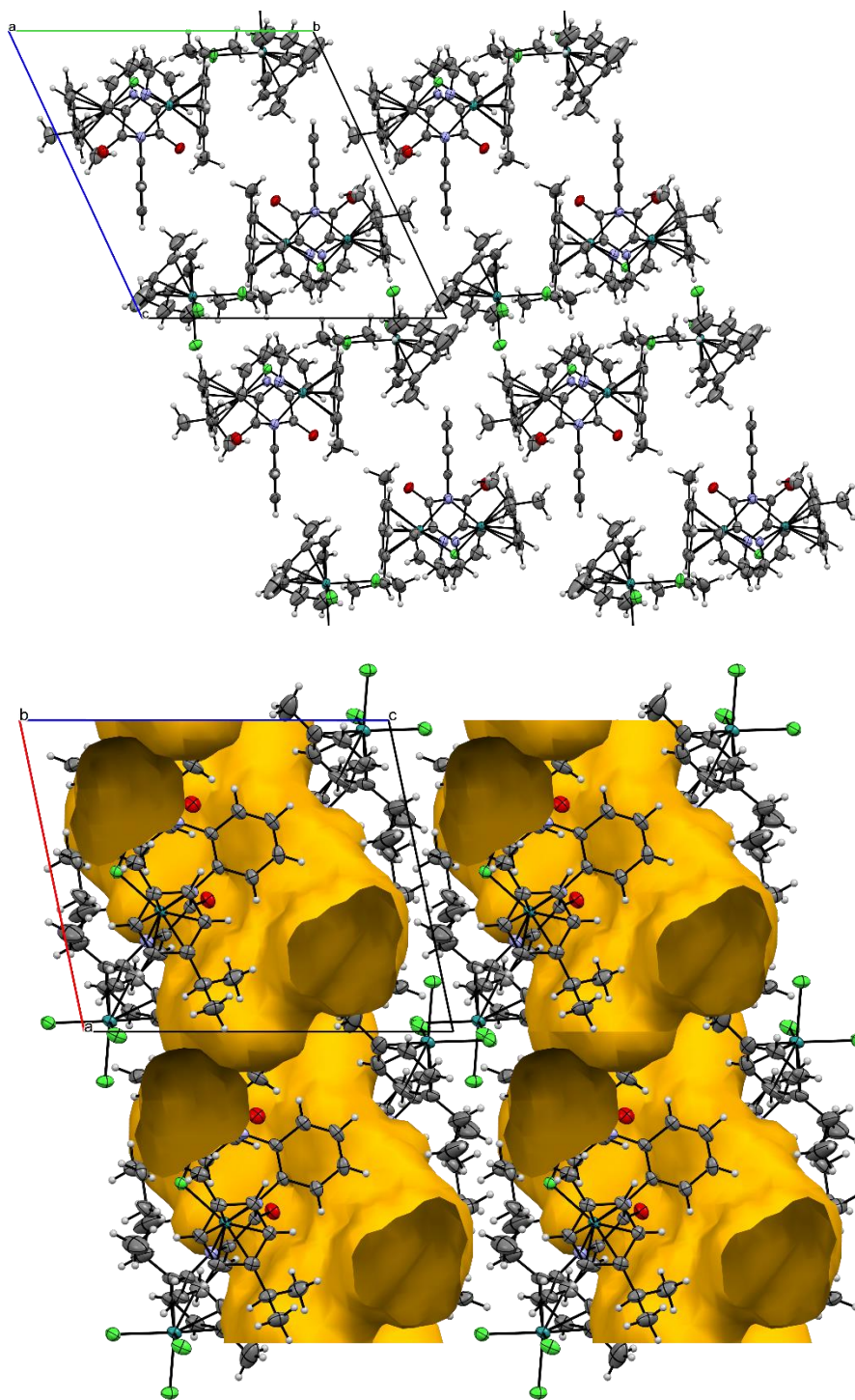


Figure S37. Molecular packing arrangement of **Ru1** viewed along *a*-axis showing two asymmetry units per unit cell (triclinic space group).

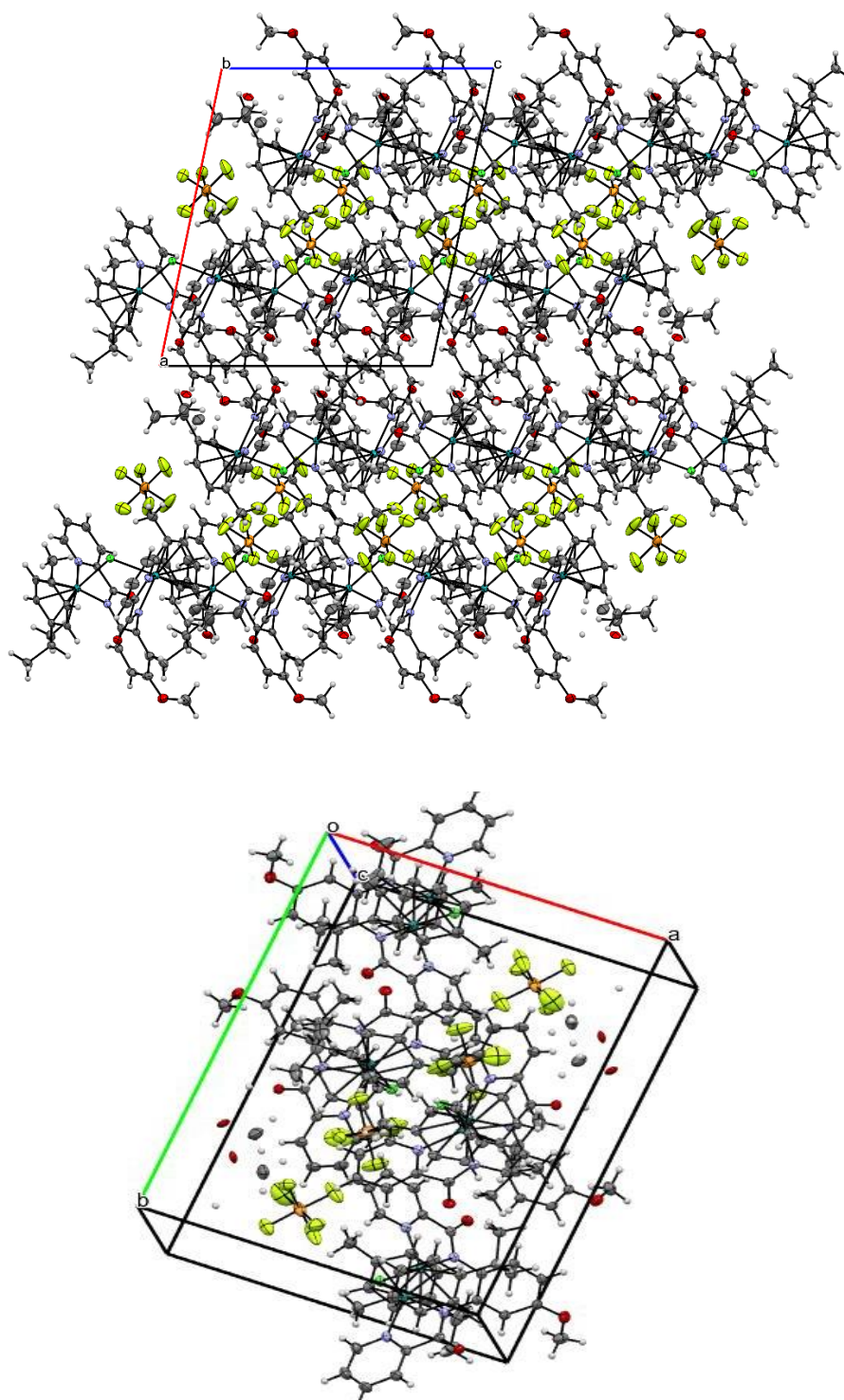


Figure S38. Molecular packing arrangement of **Ru4** viewed along *a*-axis showing four asymmetry units per unit cell (monoclinic space group).

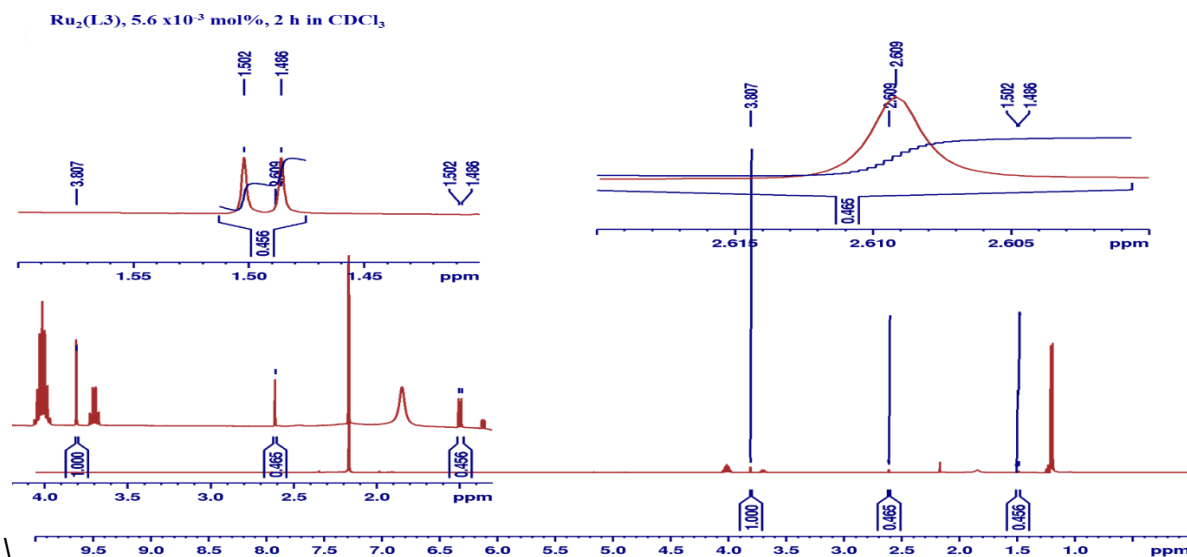


Figure S39. ^1H NMR spectrum (400 MHz, $d\text{-CDCl}_3$) of TH of acetophenone. [**Ru3**, 5.6×10^{-3} mol%] was used as catalyst]. An aliquot was taken and analysed after 2 h of reaction. The integral values of methyl protons of acetophenone and 1-phenylethanol corresponding to the percentage conversion of 53% and yield of 52% (**Figure 3**).

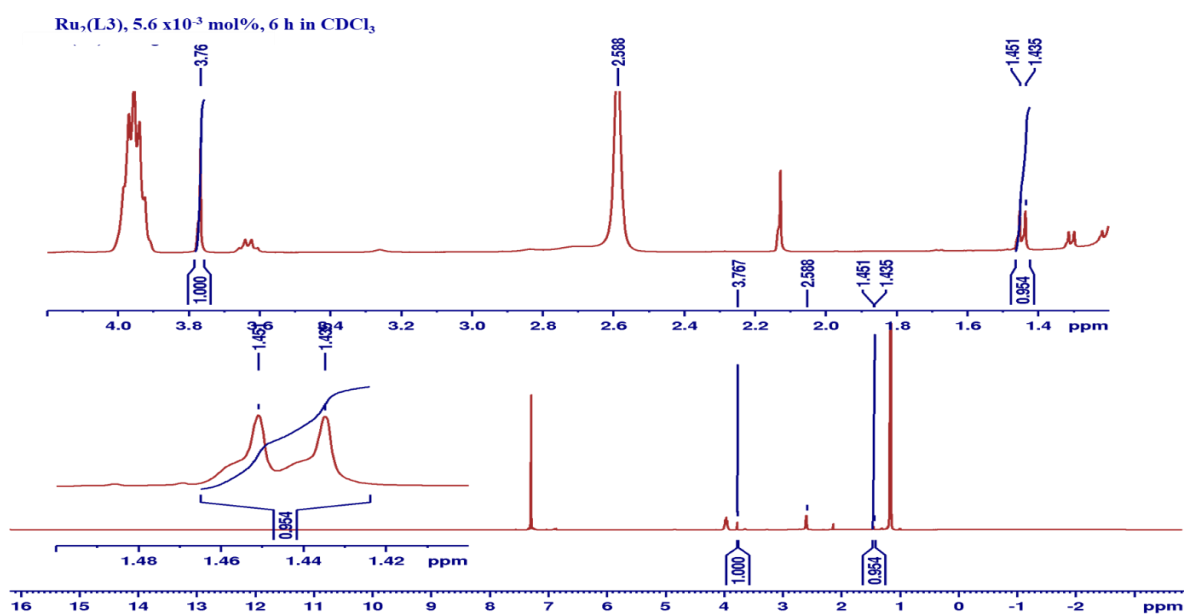


Figure S40. ^1H NMR spectrum (400 MHz, $d\text{-CDCl}_3$) of TH of acetophenone. **Ru1**, 5.00×10^{-3} mol%] was used as catalyst]. An aliquot was taken and analysed after 6 h of reaction. The integral values of methyl protons of acetophenone and 1-phenylethanol correspond to the percentage conversion of 99% and yield of 98% (**Figure 3**, **Table 3**, entry 2).

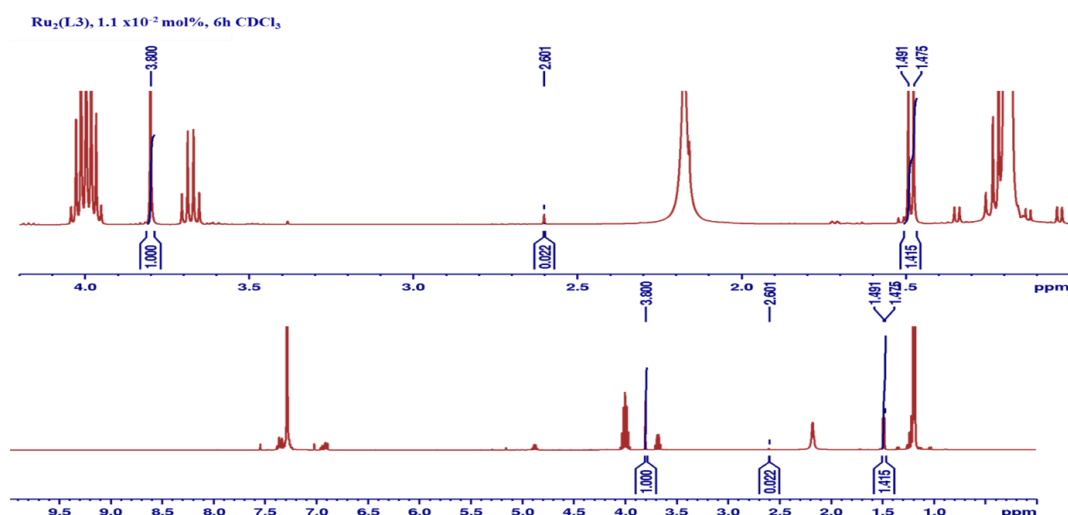


Figure S41. ^1H NMR spectrum (400 MHz, $d\text{-CDCl}_3$) of TH of acetophenone. **Ru1** was used as catalyst]. The aliquot was taken and analysed after 6 h of reaction. The integral values of methyl protons of acetophenone and 1-phenylethanol corresponding to the percentage conversion of 99% and yield of 98% (**Figure 3** and **Table 3, entry 2**).

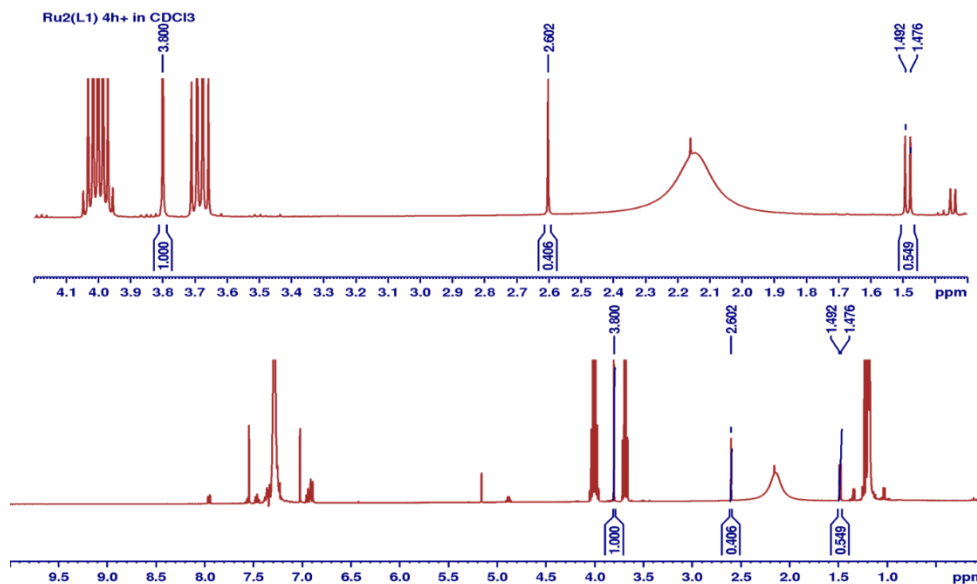


Figure S42. ^1H NMR spectrum (400 MHz, $d\text{-CDCl}_3$) of TH of acetophenone. **Ru2** was used as catalyst). An aliquot was taken and analysed after 4 h of reaction. The integral values of methyl protons of acetophenone and 1-phenylethanol corresponding to the percentage conversion of 60% and yield of 57% (**Figure 4**).

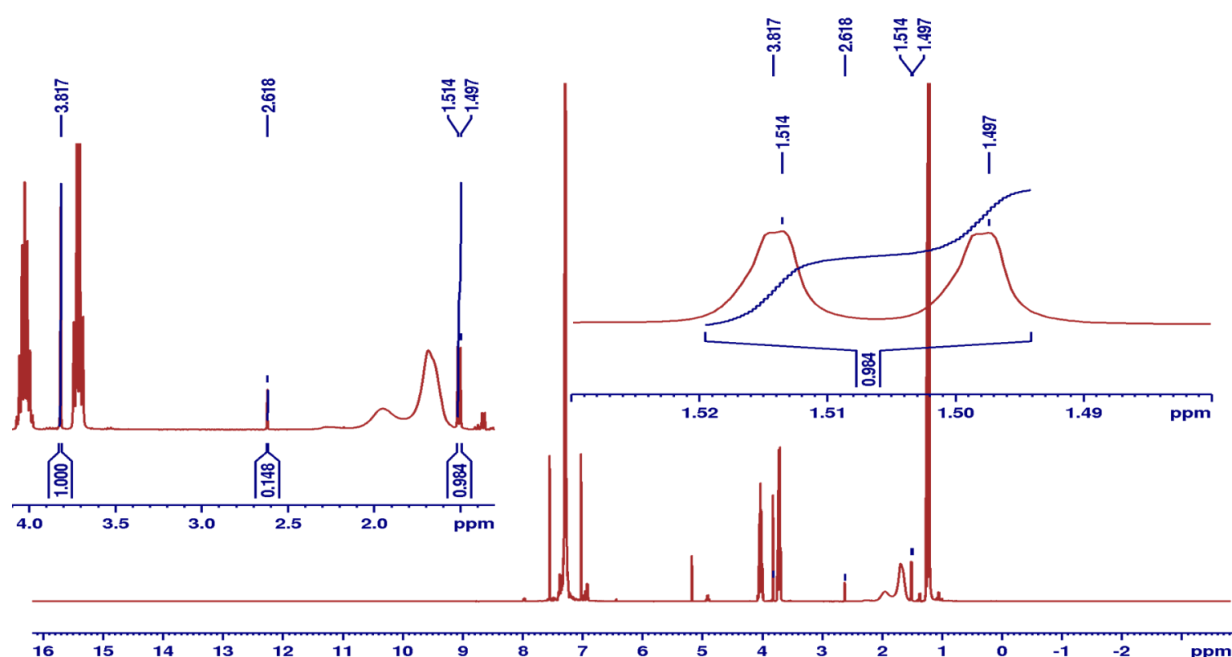


Figure S43. ^1H NMR spectrum (400 MHz, $d\text{-CDCl}_3$) of TH of acetophenone. **Ru2** was used as a catalyst). An aliquot was taken and analysed after 6 h of reaction. The integral values of methyl protons of acetophenone and 1-phenylethanol corresponding to the conversion of 86% and yield of 85% (Table 2, entry 4).

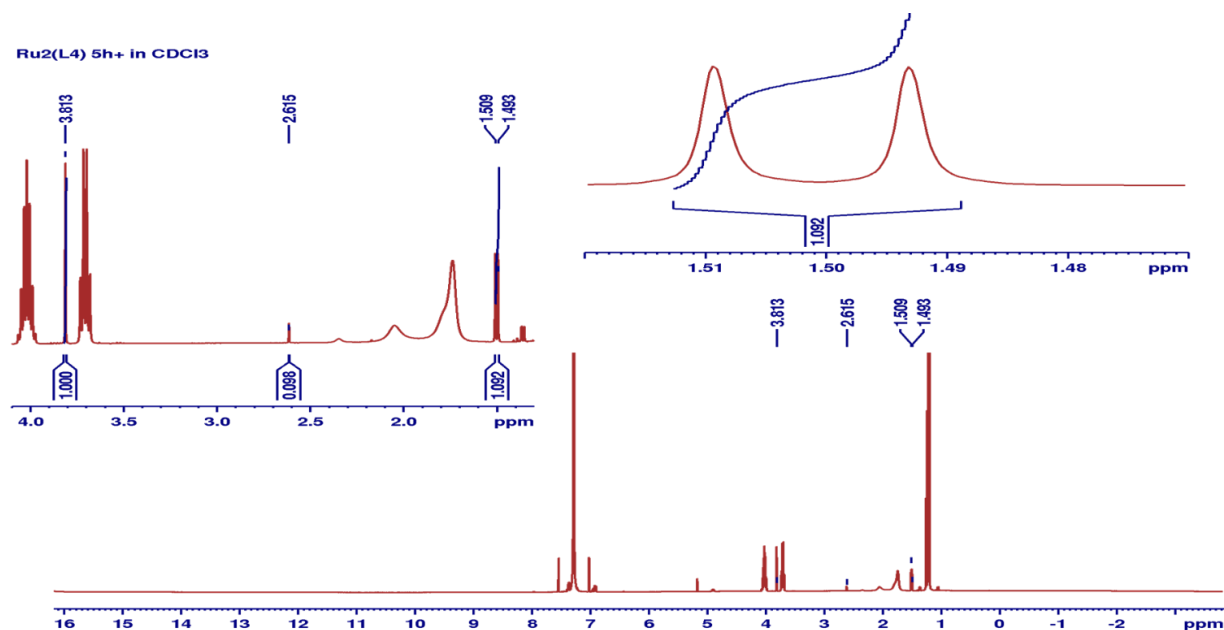


Figure S44. ^1H NMR spectrum (400 MHz, $d\text{-CDCl}_3$) of TH of acetophenone. **Ru4** was used as a catalyst). An aliquot was taken and analysed after 5 h of reaction. The integral values of methyl protons of acetophenone and 1-phenylethanol corresponding to the conversion of 92% and yield of 92% (Figure 4 and Table 3, entry 5).

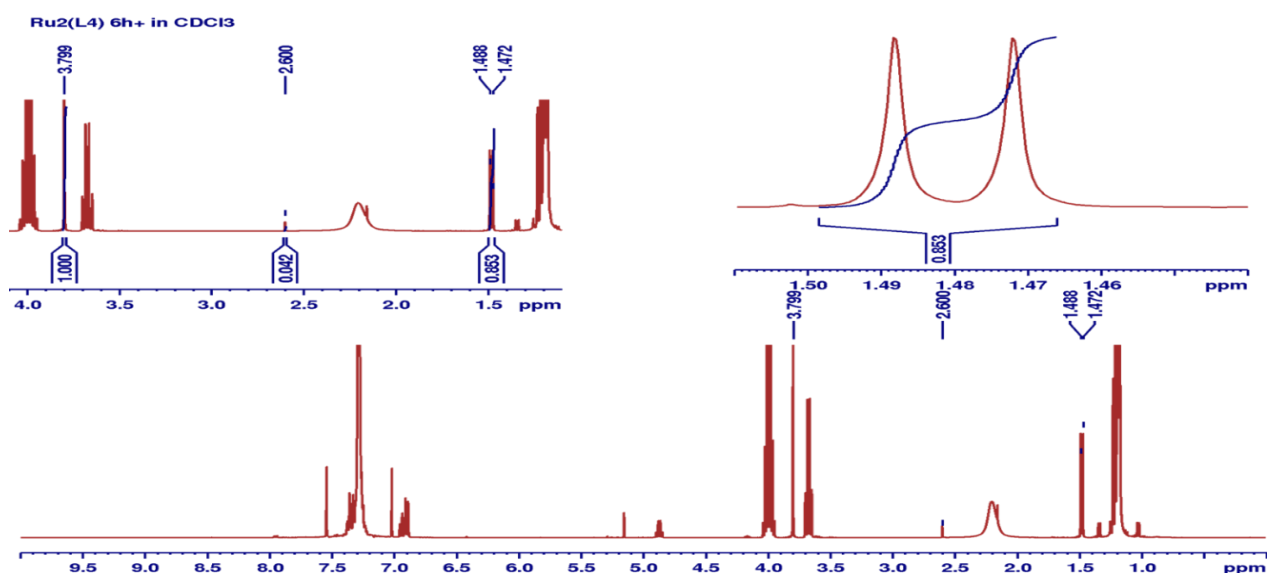


Figure S45. ^1H NMR spectrum (400 MHz, $d\text{-CDCl}_3$) of TH of acetophenone. **Ru3** was used as a catalyst). An aliquot was taken and analysed after 6 h of reaction. The integral values of methyl protons of acetophenone and 1-phenylethanol corresponding to the conversion of 96% and yield of 95% (Figure 4 and Table 2, entry 6).

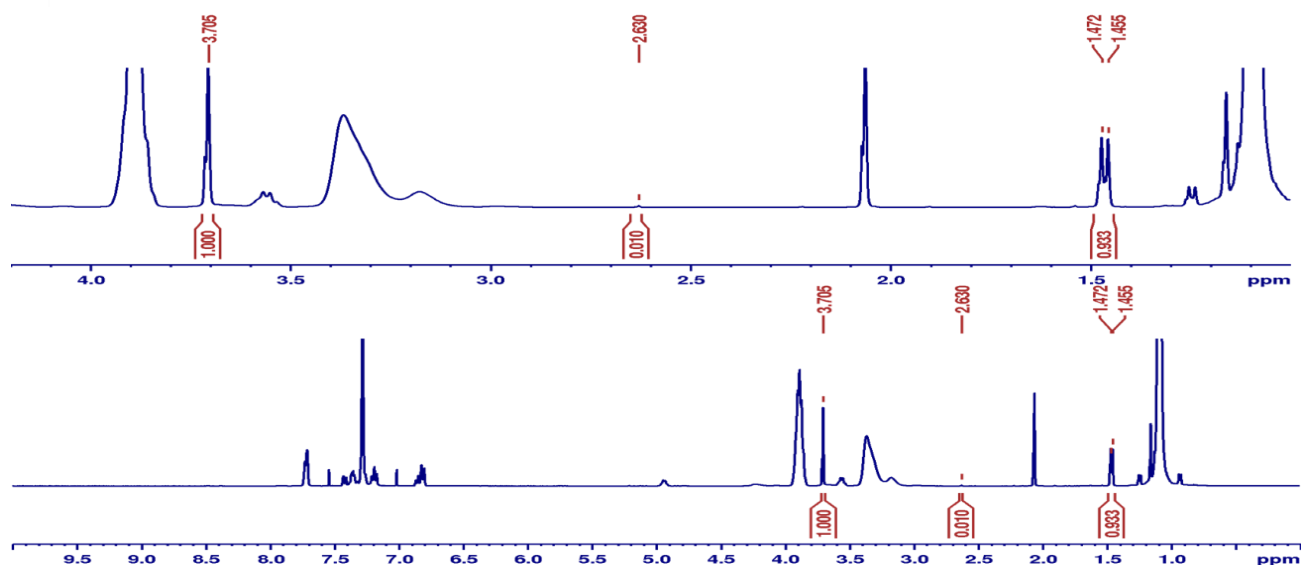


Figure S46. ^1H NMR spectrum (400 MHz, $d\text{-CDCl}_3$) of TH of 2-chloroacetophenone. **Ru2** was used as a catalyst). An aliquot was taken and analysed after 4 h of reaction. The integral values of methyl protons of 2-chloroacetophenone and the product corresponding to the conversion of 99 % and yield of 99% (**Table 4, entry 2**).

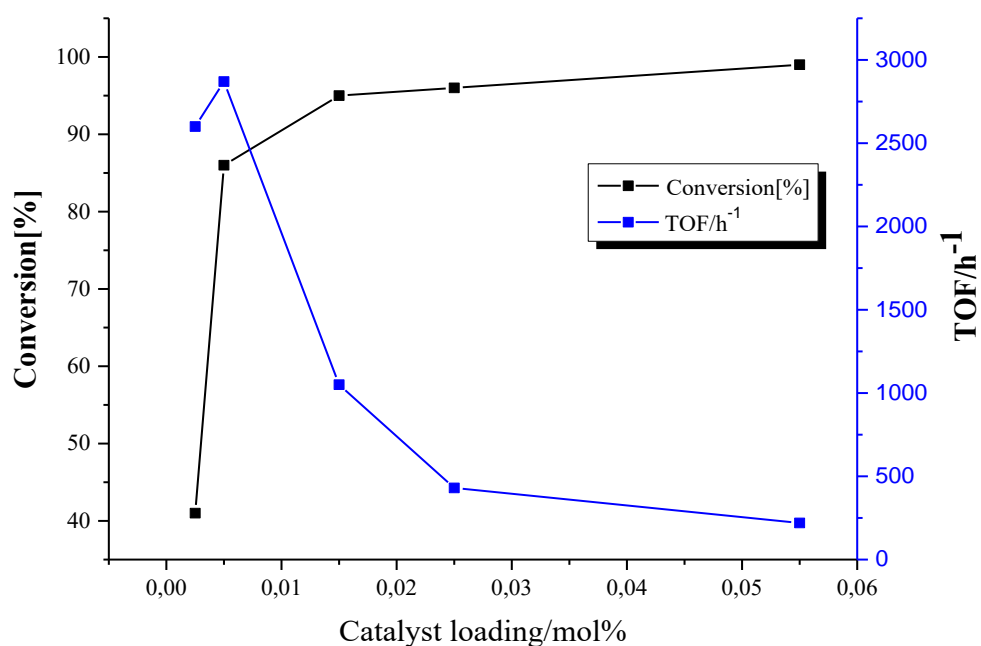


Figure S47. A plot of Conversion, TOF vs catalyst loading used to determine optimised reaction conditions.

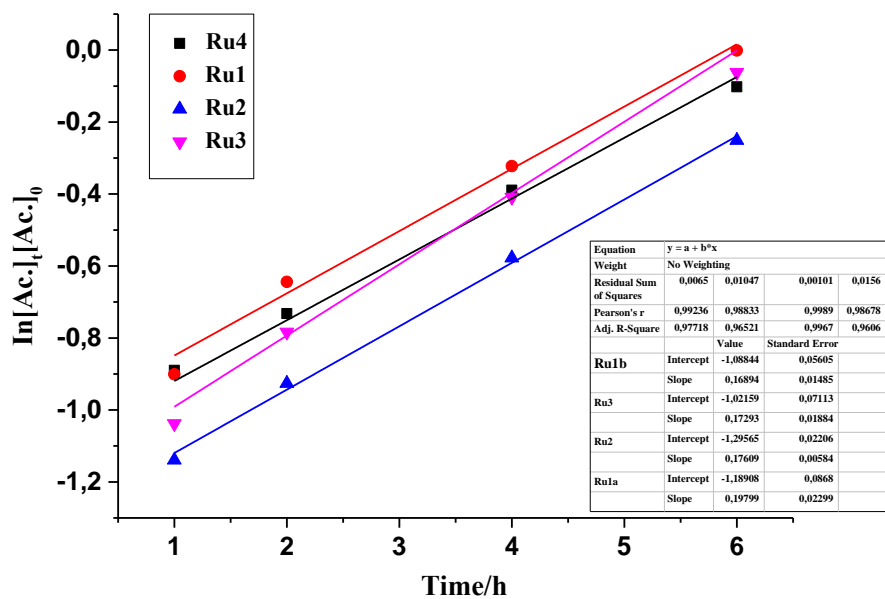


Figure S48. The plot of $\ln[Ac.]_t/[Ac.]_0$ vs time for determination of k_{ob} of the catalysts. $[Ac.]$ = concentration of acetophenone, t = time.